The Astron Astrophys Rev (1996) 7: 1–54

THE
ASTRONOMY
AND
ASTROPHYSICS
REVIEW

Cygnus A

C. L. Carilli[1,2] and P. D. Barthel[3]

[1] Leiden Observatory, Postbus 9513, 2300 RA Leiden, The Netherlands
[2] Harvard-Smithsonian Center for Astrophysics, Cambridge, MA 02138, USA
[3] Kapteyn Astronomical Institute, P.O. Box 800, 9700 AV Groningen, The Netherlands

Received October 10, 1995

Summary. Cygnus A was the first hyper-active galaxy discovered, and it remains by far the closest of the ultra-luminous radio galaxies. As such, Cygnus A has played a fundamental role in the study of virtually all aspects of extreme activity in galaxies. We present a review of jet theory for powering the double-lobed radio emitting structures in powerful radio galaxies, followed by a review of observations of Cygnus A in the radio, optical, and X-ray relevant to testing various aspects of jet theory. Issues addressed include: jet structure from pc- to kpc-scales, jet stability, confinement, composition, and velocity, the double shock structure for the jet terminus and the origin of multiple radio hotspots, the nature of the filamentary structure in the radio lobes, and the hydrodynamic evolution of the radio lobes within a dense cluster atmosphere, including an analysis of pressure balance between the various gaseous components. Also discussed are relativistic particle acceleration and loss mechanisms in Cygnus A, as well as magnetic field strengths and geometries both within the radio source, and in the intracluster medium. We subsequently review the classification, cluster membership, and the emission components of the Cygnus A galaxy. The origin of the activity is discussed. Concentrating on the nuclear regions of the galaxy, we review the evidence for an obscured QSO, also given the constraints on the orientation of the radio source axis with respect to the sky plane. We present an overview of models of central engines in AGN and observations of Cygnus A which may be relevant to testing such models. We conclude with a brief section concerning the question of whether Cygnus A is representative of powerful high redshift radio galaxies.

Key words: Galaxies: active – Galaxies: individual: Cygnus A – Radio continuum: galaxies

Correspondence to: P.D. Barthel

Introduction

Cygnus A was among the first discrete cosmic radio sources identified, using Yagi antennas, parabolic dishes, and the 'sea interferometer' (Hey, Phillips, and Parsons 1946, Hey, Parsons and Phillips 1946, Bolton and Stanley 1948, Bolton 1948; see also Bolton 1982, Slee 1994). Early interferometric observations revealed Cygnus A as a double radio source (Jennison and Das Gupta 1953), and allowed for an accurate position to be determined (Smith 1951, Mills 1952, Hanbury-Brown, Jennison, and Das Gupta 1952; see also F.G. Smith 1984). Following earlier work by Mills and Thomas (1951) including an attempt to measure the annual parallax, the accurate position was used by Dewhirst (1951) and Baade and Minkowski (1954) in their optical identification of Cygnus A as the first ultra-luminous active galaxy. The enormous energy involved was initially explained within a colliding galaxy scenario (Baade and Minkowski 1954, Minkowski and Greenstein 1954), but the double nature of the radio source, stretching outside the optical object, was puzzling.

Since its discovery, Cygnus A has played a fundamental role in the development of jet theory for powering the double structures in powerful radio galaxies. Early aperture synthesis images of Cygnus A led to the discovery of radio 'hotspots' at the source extremities (Mitton and Ryle 1969, Hargrave and Ryle 1974). As first pointed out by Hargrave and Ryle (1974), the radiative lifetimes of the relativistic electrons in these hotspots ($\approx$ few$\times 10^4$ years) are less than the light travel time from the nucleus to the hotspot ($\approx 1.5 \times 10^5$ yrs, for H_0 = 100 km sec^{-1}Mpc^{-1}), hence requiring continuous injection of a population of relativistic electrons at the hotspots. This conclusion led to the 'beam' or 'jet' model for powering double radio sources (Blandford and Rees 1974, Scheuer 1974). The jet model also avoids the dramatic expansion losses inherent in single-burst 'plasmon' models for extended structures in radio galaxies (van der Laan and Perola 1969, Longair, Ryle, and Scheuer 1973, DeYoung and Axford 1967). The Cygnus A jet itself was suggested in early VLBI observations of the nucleus (Kellermann et al. 1975, Kellermann et al. 1981, Linfield 1982), and finally revealed in detail by the first high dynamic range images of the source with the VLA (Perley, Dreher, and Cowan 1984).

More generally, Cygnus A has played a key role in the field of radio-loud active galaxy research (e.g., Burbidge, Burbidge and Sandage 1963). It was among the first such galaxies to be detected, and is by far the closest of the ultra-powerful radio galaxies. Fig. 1 shows the classic 'Malmquist bias' in the flux limited 3C sample of powerful radio galaxies (Laing et al. 1983). These are all high luminosity (spectral luminosity $\geq 10^{33}$ ergs sec^{-1} Hz^{-1} for H_0 = 75 km sec^{-1}Mpc^{-1} at rest frequency 178 MHz), edge-brightened, Fanaroff-Riley class II radio galaxies (FRII or 'classical doubles'; Fanaroff and Riley 1974)[1].

The position of Cygnus A, 3C 405, on this redshift-luminosity diagram is unique: a very high radio luminosity – more than two orders of magnitude above the standard FRI-FRII break, with a very low redshift (z = 0.0562, Stockton et al. 1994). Cygnus A is about 1.5 orders of magnitude more luminous than any other source at $z \leq 0.1$. Indeed the next closest source of similar luminosity is 3C 295, at z = 0.46, and most sources with luminosities similar to Cygnus A are located at $z \approx 1$. Hence, Cygnus A may provide an example to separate the effects of radio luminosity and epoch in the currently topical field of high redshift radio galaxies (McCarthy 1993).

[1] For comparison, radio galaxies of lower luminosity typically show edge-darkened morphologies, and are called FRI sources.

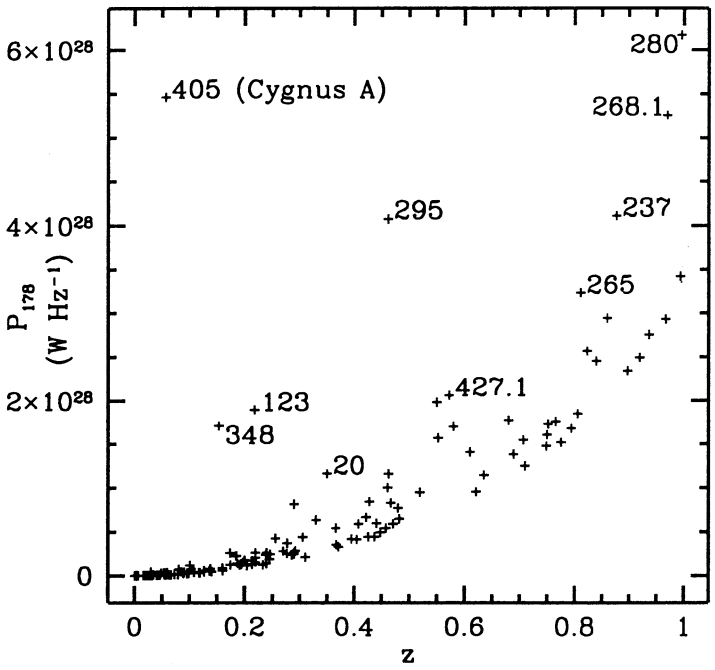

Fig. 1. The radio power–redshift relation for the 3C sample of $z < 1$ FRII radio galaxies, calculated using H_0 = 75 km sec^{-1}Mpc^{-1} and q_0 = 0.5 (from Stockton and Ridgeway 1996). The more luminous sources are labeled

Its enormous radio flux density has allowed for high S/N radio observations from the early days of radio astronomy. This is in contrast to the optical and infrared where high S/N observations of the faint galaxy require sensitive detectors and large apertures, and progress was slower. However, renewed interest in the optical and near infrared properties arose with the proposition that the Cygnus A galaxy might harbour a QSO in its nucleus (Pierce and Stockton 1986, Tadhunter et al. 1990, Vestergaard and Barthel 1993).

Following are some conventions used in this review. We use h = H_0/100 km sec^{-1}Mpc^{-1} and q_0 = 0.5, implying a luminosity distance for Cygnus A of 172/h Mpc, and an angular size distance of 154/h Mpc such that $1'' = 0.75\ h^{-1}$ kpc. Spectral index, α, is defined as a function of frequency, ν, and intensity, I(ν), as: I(ν) $\propto \nu^{\alpha}$. We use cgs units unless stated otherwise. The symbol 'c' is used for the speed of light.

Some basic observational parameters for Cygnus A are listed in Table 1. This review is organized by physical question, starting with the radio source. We begin with a short review of jet theory for powerful radio galaxies. We then discuss the radio continuum morphology and spectra of the jets, hotspots, and lobes, followed by a review of internal and foreground magnetic fields (as inferred from the radio data). The subsequent section discusses the X-ray cluster and the interaction between the radio source and the cluster gas. We then summarize the optical and infrared properties of the Cygnus A galaxy and discuss in detail the active nuclear regions, including the question of a possible hidden quasar in Cygnus A. We present an overview of models of central engines in AGN and observations of Cygnus A which may be relevant

Table 1. Cygnus A Basic observational parameters

z	0.0562
P^a_{178}	3.0×10^{35} h^{-2} erg sec^{-1} Hz^{-1}
L^b_R	5.0×10^{44} h^{-2} erg sec^{-1}
D^c_R	103 h^{-1} kpc
$S^d_{core,5}$	0.75 Jy/beam
m^e_R	14.48
L^f_{opt}	4.7×10^{44} h^{-2} erg sec^{-1}
$m^g_{K,nucl.}$	16.2
$S^h_{60\mu}$	2.85 Jy
$L^i_{X,nucl.}$	6.2×10^{44} h^{-2} erg sec^{-1}
$L^j_{X,gas}$	6.8×10^{44} h^{-2} erg sec^{-1}
$T_P(CO)^k$	< 1.3 mK

[a]Spectral luminosity at 178 MHz (rest-frame frequency).
[b]Total radio luminosity between 10 MHz and 400 GHz, derived using a two component powerlaw spectrum with index -0.7 from 10 MHz to 2 GHz, and -1.2 from 2 GHz to 400 GHz. Note that the spectrum turns over sharply below 10 MHz (cf. Baars et al. 1977).
[c]Radio source size, defined by separation of hot spots A and D.
[d]Nuclear radio source peak surface brightness at 5 GHz, 0.4″ (FWHM) resolution.
[e]Apparent R magnitude in a Gunn-Oke aperture, corresponding to 23″ at the distance of Cygnus A.
[f]Bolometric optical luminosity assuming a G0 stellar spectrum.
[g]Apparent K magnitude of nucleus, as derived by Djorgovski et al. (1991).
[h]60 μm flux density of Cygnus A, from Golombek, Miley, and Neugebauer (1988).
[i]Luminosity of the nucleus between 2 and 10 keV from Ueno et al. (1994).
[j]Luminosity of the hot cluster gas between 2 and 10 keV from Ueno et al. (1994).
[k]CO(1–0) emission limit from Mazzarella et al. (1993).

to testing such models. We conclude with a brief section concerning the question of whether Cygnus A is representative of powerful high redshift radio galaxies. Our literature search is complete to mid 1995, and the review includes views and results presented at the May 1995 Cygnus A Workshop held at NRAO, Green Bank, WV (see Carilli and Harris 1996).

Jet theory

The standard model

When imaged with adequate sensitivity and resolution powerful (FRII) double radio galaxies always show four basic morphological components: at the center of the parent optical galaxy is a compact, typically flat spectrum, high surface brightness 'core' component. Extending from this compact component to the source extremities are highly elongated radio emitting structures, or 'jets'. The jets usually end at, or point towards, high surface brightness 'hotspots' at the extremities of the radio source. The region in between the radio hotspots is filled with extended, low surface brightness, often filamentary emission, known as 'radio lobes'. These four components are all clearly evident on the 5GHz radio image of Cygnus A made with the VLA (Fig. 2).

The standard physical model explaining and relating these four morphological structures is known as the 'jet model' for powerful radio galaxies, as first suggested in Longair et al. (1973) and Hargrave and Ryle (1974), and worked out in detail in

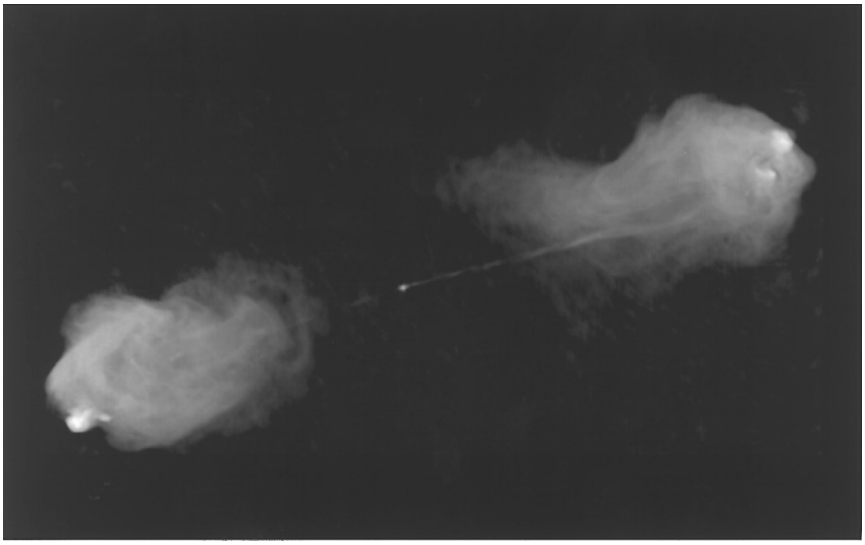

Fig. 2. A greyscale representation of the image of Cygnus A at 5 GHz with $0.4''$ resolution made with the VLA (courtesy R. Perley)

Blandford and Rees (1974) and Scheuer (1974). A seminal review of this topic can be found in Begelman et al. (1984), and we briefly summarize the basics of this model.

The radio core corresponds to the 'central engine' – the ultimate source of energy responsible for the double radio structures. Unfortunately our understanding of the physics of central engines in AGN remains limited, mostly due to the lack of direct observational constraints. For reviews of central engines in AGN see Begelman et al. (1984), Begelman (1993), Miller (1985), and Wiita (1991). The one certain fact about central engines is that they generate a tremendous amount of energy, $>> 10^{45}$ ergs $\sec^{-1}$ in a very small volume ($<<$ 1 pc radius). Some, or perhaps much, of this energy can be released in the form of highly collimated, supersonic, and probably relativistic, outflows of plasma and magnetic field – the radio 'jets'. For reviews of various aspects of jets in powerful radio galaxies see Bridle and Perley (1984), Bridle and Eilek (1985), Zensus and Pearson (1990), Hughes (1991), Burgarella et al. (1993), Zensus and Kellermann (1994), and Röser and Meisenheimer (1995).

The jets in FRII sources propagate relatively unhindered until they terminate in a strong shock on impact with the external medium. At this point the jets convert some, perhaps most, of their bulk kinetic energy into relativistic particles (through first order Fermi acceleration), and magnetic fields (through simple shock compression, or more complex dynamo processes in the turbulent post-shock flow). This post-jet shock fluid emits copious radio synchrotron radiation resulting in the high surface brightness radio 'hotspots'. Reviews of physical processes in hotspots can be found in Röser and Meisenheimer (1989). The high pressure shocked jet material then expands out of the hotspot transversely inflating a synchrotron emitting 'cavity' in the ambient medium of waste-jet material – the radio 'lobe'.

The outline above applies to the radio emitting structures. A second aspect of this model is the effect of the radio source on the ambient medium. Fig. 3A shows a schematic of the effect an expanding radio source will have on the ambient medium on large scales, while Fig. 3B shows a detail of the terminal jet shock structure. At

the jet terminus two shocks are formed: the jet shock, or Mach-disk, which effectively stops the incoming jet, and the standoff, or bow, shock which acts to accelerate and heat the ambient medium. The two shocked fluids (jet and ambient) meet in pressure balance along a contact discontinuity. Observational evidence suggests that the contact discontinuity is largely stable to mixing (Carilli, Perley, and Dreher 1988).

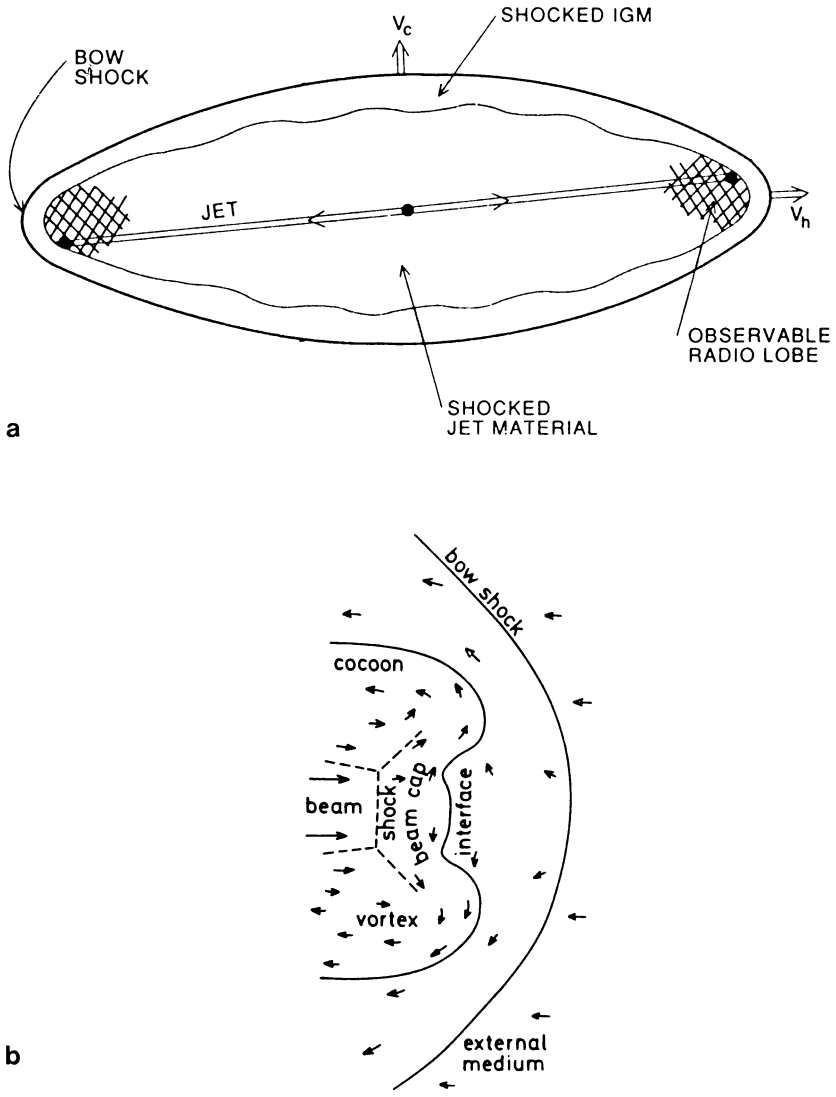

Fig. 3A,B. A schematic representation showing the effect an expanding radio source will have on the external medium. Fig. A is reproduced from Begelman and Cioffi (1989), and shows the expected large-scale distribution of shocked ambient gas enveloping the radio lobes. Figure B is reproduced from Smith et al. (1985) and shows a detail of the expected double-shock structure at the jet terminus. The interface is the contact discontinuity between shocked jet material and shocked intracluster material (ICM). The beam shock and cap correspond to the radio hotspots, and the cocoon corresponds to the radio lobe

Hence the overall picture is one of a radio source being enveloped by a 'sheath' of shocked ambient medium. If the jet direction is roughly constant over time the radio lobe grows as a roughly 'cigar-shaped' cavity with the principal active surface being associated with the high radio surface brightness regions at the lobe extremities. In this model the shocked intracluster medium forms a thin dense sheath in the vicinity of the hotspots (since this is the location of the 'driving piston'), and a much broader, less dense sheath in the vicinity of the tails of the radio lobes.

Simulations

Significant insight into the physics of extragalactic radio sources has come through numerical simulations. Reviews of such results can be found in Norman (1989), Williams (1991), and Clarke (1990, 1992). We briefly consider some of the more important results as they apply to sources such as Cygnus A.

The basic structure of supersonic jets, hotspots, and radio lobes were delineated in the early work of Norman et al. (1982). These two-dimensional, axisymmetric hydrodynamic simulations showed the development of the double shock structure at the jet terminus (Mach disk and bow shock), and the evolution of the radio lobe, or 'cocoon' of shocked jet material enveloping the jet. A fundamental conclusion from these simulations was that well developed radio lobes, with widths much larger than the jet width, only result from very under-dense jets (η = jet density/external density < 0.1), with high internal Mach numbers ($M > 6$). In this case the advance speed of the terminal Mach disk is much less than the jet speed thereby requiring a 'waste-bin' for the shocked jet material, i.e. the radio lobe. The beam stability is greatly enhanced by the development of this low-density cocoon within which the jet is over-dense, and hence essentially ballistic (Icke 1991). The pressure gradient between the hotspot and lobe may drive a 'back-flow' of waste jet material towards the nucleus.

Non-axisymmetric 'slab', or full three-dimensional (3D), simulations have answered the interesting issue of multiple hotspots in powerful radio galaxies by allowing for jets which alter direction on time-scales shorter than the radio source lifetime (Williams and Gull 1985, Hardee and Norman 1990, Cox et al. 1991), lending credence to the simple 'dentist drill' idea of Scheuer (1982). Such models also result in larger lobe-to-jet width ratios than in axisymmetric models, since the working surface of the jet acts over a much larger area at the head of the lobe as a function of time.

Simulations including dynamically passive magnetic fields result in total and polarized intensity distributions which match the observations reasonably well (Clarke 1992, Mathews and Scheuer 1991), including 'hamburger hotspots' at the terminal Mach disks, high fractional polarizations along source edges, and filamentary structures in radio lobes. Simulations involving dynamically important fields result in a prominent 'nose-cone' of emission beyond the terminal Mach disk, and no development of a radio cocoon (Clarke 1992; Clarke et al. 1989, Lind et al. 1989). Neither of these features is consistent with the observed structures in sources such as Cygnus A. Overall, Clarke (1992) concludes that most of the structures of FRII radio galaxies can be explained reasonably within the context of 3D simulations of light, fast jets which alter direction by small angles on fairly short time-scales, and within which the magnetic fields are not dynamically dominant.

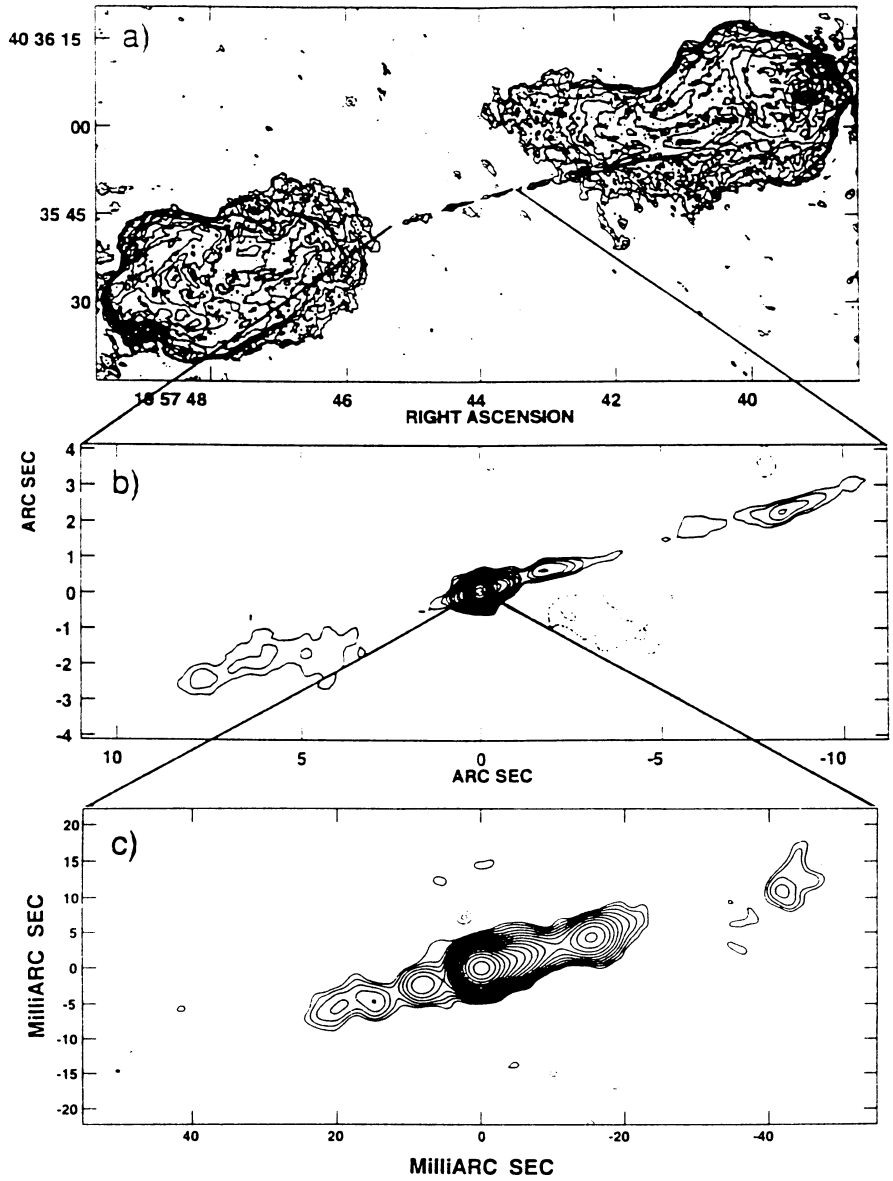

Fig. 4. Contour images of the Cygnus A radio jet on various scales, reproduced from Sorathia et al. 1996. The top image shows kpc-scale radio source at 5 GHz with a resolution of $0.4''$. The contour levels are a geometric progression in $\sqrt{2}$, which implies a factor two rise in surface brightness every two contours. The first level is 2.25 mJy/beam. The middle image is of the inner kpc-scale jet of Cygnus A with the same contouring as above. The bottom image shows the pc-scale jet of Cygnus A at 3mas resolution (FWHM). The contouring scheme is the same as above, but the first contour level is 1 mJy/beam

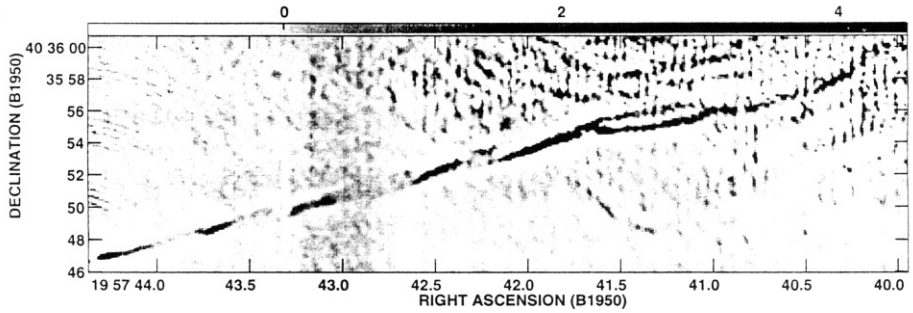

Fig. 5. A high pass filtered image of the jet in Cygnus A made from an image at 5 GHz, 0.4″ resolution, by subtracting a smoothed version of the same image from the full resolution image

The jets in Cygnus A from pc- to kpc-scales

Images: bends and knots

Jets and related structures in extragalactic radio sources are the largest coherent physical structures in the universe, obtaining sizes of order 1 Mpc in some cases (DeYoung 1991). The remarkable collimation and stability of these jets remains somewhat of a mystery and a marvel (Icke 1991, Birkinshaw 1991).

A composite of images showing the Cygnus A jets at various scales is shown in Fig. 4. A jet towards the northwest lobe is clearly detected on both pc- and kpc-scales. The counterjet towards the southwest lobe is fainter, but also evident on both kpc-scales (Carilli et al. 1996), and on pc-scales (Krichbaum et al. 1996, Sorathia et al. 1996). The jet is well collimated and directed starting on scales $\leq$ 0.6 mas, and continuing to 60″. Between 2 mas and 20 mas the jet position angle is 284°$\pm$2°. The kpc-scale jet also has a position angle of 284°$\pm$1° from 1″ to 25″ from the nucleus. The counterjet on kpc-scales has a position angle of 108°$\pm$2°, implying that the jet and counterjet are apparently misaligned (with respect to reflection symmetry) by 4°.

Out to 25″ the jet is composed of a series of elongated knots, as can be seen in Fig. 5. The knots are all oriented at an oblique angle of about 7° to the jet axis. The knots are fairly regularly spaced by about 7″. Beyond 25″ the jet appears to 'bifurcate', and gently curves towards the south, and then northward again, eventually becoming indistinguishable from filamentary structure in the lobe. Rudnick et al. (1994) and Carilli et al. (1989a) present images of the counterjet in Cygnus A revealing a dramatic bend by about 30° over a distance of about 30″ before it enters the primary hotspot E in the southern lobe.

Gradual bends in radio jets could result from pressure gradients in the lobes, eg. due to large-scale turbulent eddies in the lobe back-flow (Icke 1991, Cox et al. 1991, Hardee and Norman 1990), or from jet instabilities (Hardee and Clarke 1992), or simply indicate the direction of ejection from the central engine. In the latter case the flow proceeds radially from the nucleus, and not along the observed jet structure. In Cygnus A there is marginal evidence that the magnetic field lines project parallel to the gradual curvature of the jet in the region between 25″ to 45″ from the nucleus. Such a field morphology is expected in the case when the jet flow is parallel to the observed curvature.

There have been many explanations proposed for knots in jets in powerful radio galaxies (Williams 1991), including internal shocks due to surface instabilities or changing surface pressure (Norman et al. 1982, Falle and Wilson 1985, Birkinshaw 1991), variations in the jet velocity (Rees 1978), bow shocks due to collisions with small, dense clouds (Blandford and Königl 1979), or oscillations between magnetic and thermal pressure dominance in an axisymmetric jet with a 'pinching' toroidal magnetic field (Chan and Henriksen 1980). Two characteristic of the knots in Cygnus A which any model must address are that the knots are clearly not axisymmetric, and that they have a fairly regular pattern in terms of length, separation, and pitch angle.

One model which predicts a regular, non-axisymmetric pattern of knots in a jet has been presented by Königl and Choudhuri (1985). They calculate the expected surface brightness distribution of a pressure confined, magnetized jet which has relaxed to a 'force-free' magnetic field configuration, i.e., no Lorentz force on the plasma. Their jet has a series of oblique knots separated by about five jet radii. They suggest that the energy supply for the synchrotron emitting plasma in jets is that dissipated in current sheets in field reconnection regions during the relaxation of the fields to the force-free configuration.

Hardee and Clarke (1992) present a strictly hydrodynamic 3D simulation of a pressure matched, high Mach, light jet, driven with small amplitude precession at the origin (to break axisymmetry). Their jet develops twisted filamentary surface structures due to higher order ('fluting' mode) Kelvin-Helmholtz surface instabilities, and an elliptical distortion in the jet cross-section, culminating in a helical bifurcation of the flow. They conclude that the edge-brightened, twisted appearance of the Cygnus A jet at $30''$ from the nucleus is reasonably modeled by this coupled helical-elliptical mode.

The results of Hardee and Clarke (1992) have been generalized to include magnetic fields by Hardee and Clarke (1995). Using a a 3D magnetohydrodynamical (MHD) simulation of a dense, supermagnetosonic jet, they find that the jet can maintain both a helical twist and an elliptical distortion of large amplitude over a distance ≥ 60 jet radii without disrupting. The predicted jet radio morphology includes a series of oblique filaments crossing the jet at regular intervals, much like that seen for the Cygnus A jet. A detailed comparison between this simulation and the observed structures of the Cygnus A jet by Hardee (1996) yields: $\gamma M_j \approx 10$ and $\gamma^2 \eta_j \approx 6$, where γ is the jet Lorentz factor, η_j is the density ratio between the jet and the radio lobe, and M_j is the jet magneto-sonic Mach number.

Opening angle, stability, and confinement

An important constraint on jet physics is the opening angle. For a free jet the opening angle, θ will equal 2ϕ, where ϕ is the Mach angle defined by: $\tan(\phi) = (\gamma M_j)^{-1}$, where M_j = jet Mach number, and γ = jet Lorentz factor. Any oblique shock in the jet due to a disturbance at the surface will also have the Mach angle relative to the jet axis. Likewise, turbulent boundary layers grow at the Mach angle unless prohibited for example by internal magnetic fields. Hence, a high Mach number jet has an effective 'rigidity' since edge-effects are limited to propagate into the jet at the Mach angle (DeYoung 1991).

On pc-scales the jet is resolved transversely with a constant (deconvolved) FWHM = 2.2 mas from 4 mas to 20 mas, suggesting a confined jet (Carilli, Bartel, and Linfield

1991). The minimum pressure in jet knots at radii of a few pc are of order 10^{-6} dyn cm^{-2}, which is below the expected pressures in the ambient medium in these regions, as discussed below. Hence the pc-scale jet could be pressure confined although the possibility of magnetic focusing remains attractive in order to explain such a well collimated outflow.

On kpc-scales the opening angle of the jet in Cygnus A can be determined either from the evolution of the FWHM of the knots in the jet out to $20''$, or from the edges defined by the low surface brightness inter-knot emission in the high pass filtered image. In both cases the opening angle derived is $\approx 1.6^\circ$ (Carilli 1996). For a free non-relativistic jet, the implied Mach number is 72. For a free relativistic jet filled with relativistic fluid the internal sound speed is $c/\sqrt{3}$, hence $M_j = \sqrt{3}$ and for Cygnus A the implied Lorentz factor is: $\gamma = 40$. This is well above the range measured for superluminal quasars (e.g., Porcas 1987).

Perhaps the most reasonable conclusion is that the Cygnus A jet is confined. Perley et al. (1984) point out that the Cygnus A jet morphology is consistent with regions of larger opening angle ($\approx 5^\circ$), and a constant width jet in between (full width to 10% of peak $\approx 1.1''$), implying a confined jet. Even for a confined jet, oblique ridges may indicate the Mach number of the flow if they arise due to disturbances at the jet wall. The Cygnus A jet knots are oriented at roughly 7° to the jet axis, which if taken as the Mach angle, implies: $M_j = 8$. Lastly, there is the simple fact that the jet must widen from pc- to kpc-scales. Using the first resolved jet knot as an indicator of opening angle from the core leads to: $M_j \leq 13$.

The simplest means of jet confinement is external pressure. Perley et al. (1984) point out that minimum energy pressures in the jet are about an order of magnitude greater than in the lobes, thereby requiring an alternative means for jet confinement, if minimum conditions apply. Below we review X-ray and optical observations which suggest that the lobes may be over-pressured relative to equipartition values by just this amount and hence that pressure confinement may still be viable.

A number of authors have suggested confinement of current carrying jets via the 'plasma-pinch' mechanism due to toroidal fields surrounding the radio jet (Chan and Henriksen 1980, Bridle, Chan and Henriksen 1981, Bicknell and Henriksen 1980, Benford 1985, Siah 1985). This mechanism is notoriously unstable although it might be stabilized by longitudinal fields in the jet, or by a hyper-Alfvenic jet velocity.

One of the more interesting observational results concerning the jet in Cygnus A comes from the optical imaging of the inner $5''$ of the galaxy with HST by Jackson et al. (1994). They find that the jet passes through a 'channel' in the line emitting gas about $1''$ from the nucleus. This channel is also seen in deconvolved ground-based images (Vestergaard 1992, Stockton et al. 1994), and it has been confirmed with more recent HST images of Cygnus A (see Fig. 6) presented in Cabrera-Guerra et al. (1996). These authors do not find evidence for increased reddening at the position of the gap, and hence argue that the gap is not simply a fortuitous projection of a dust filament at the position of the radio jet. Jackson et al. (1994) and Cabrera-Guerra et al. (1996) suggest that the jet has 'blasted' a path through the emission line clouds. The shocked clouds cool quickly, and are subsequently photo-ionized by radiation from the (hidden) active nucleus. This morphology implies that the radio source has not completely evacuated its environments, at least within a few arcseconds of the nucleus. This is consistent with the simulations of Williams (1991) of a jet propagating through an atmosphere of decreasing density, in which case the inner part of the lobe gets 'squeezed' by the high pressures in the central regions, leaving a 'naked jet' in

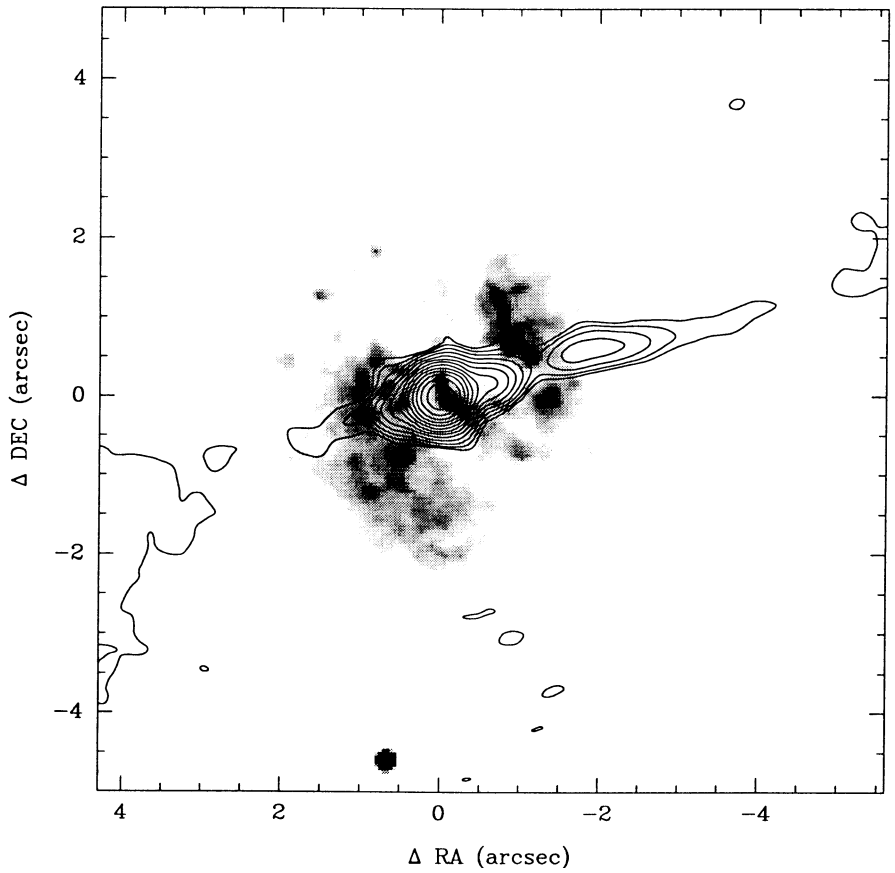

Fig. 6. The contours show the inner kpc-scale jet in Cygnus A at 5 GHz, 0.4″ resolution. The grey-scale shows an HST image (resolution $\approx$ 0.1″) of Cygnus A using the WFPC2 F622W filter, reproduced from Cabrera-Guerra et al. (1996). Note that the radio jet passes through a gap in the optical line emission

the inner regions, in direct contact with the external medium. The pressure in the line emitting gas is comparable to the minimum energy value in the jet allowing for pressure confinement of this 'naked jet'.

However, there are a number of problems with the above model. First is the general problem of stability of a light, pressure confined jet (Birkinshaw 1991). Second, if the line clouds are moving at $\geq$ few hundred km sec^{-1} they will cross the jet on a time-scale of order 10^6 yrs, thereby further complicating the issue of jet stability. And third, in order to observe a gap due to the jet in the projected line emission the gas distribution must have a rather contrived geometry. A flattened, or disk-like, geometry for the line emitting gas is precluded since the expected deficit due to a small hole in a large disk, as seen in projection, would be small. The observed gap requires the gas be in a linear filament which happens to get 'cut' by the jet.

Overall, it may be simplest to assume that the jets in Cygnus A are external pressure confined on pc- and kpc-scales with a free-expansion zone in between. The pc-scale jet is under-dense relative to its environments, and hence stability becomes a concern. The same concern holds for the jet-cloud interaction region seen at a distance

of ≈ 1 h^{-1} kpc from the nucleus. However, beyond ≈ 10 h^{-1} kpc from the nucleus the jet would be over-dense relative to the confining medium (the radio lobes), leading to the relatively stable situation of a supersonic, pressure matched, ballistic jet from ≈ 10 h^{-1} kpc to the hotspots. The single requirement of this model is that the lobes be over-pressured relative to minimum energy – an assumption that agrees with other observational aspects of the Cygnus A galaxy, as discussed below.

Velocity and composition

The proper motion of features in the pc-scale jet has been measured directly implying a value $\approx 0.5c$ h^{-1} for the projected jet velocity. Whether this is simply a pattern speed or the true flow velocity is still unknown, as is the inclination angle with respect to the sky plane. Estimates of the velocity of the jet on kpc-scales are even more problematic, but there are a few indirect methods that have been used, which we review. In this section we assume h = 0.75, both for simplicity, and because the calculations are at best order-of-magnitude.

An estimate of the jet velocity can be obtained by considering the rate of bulk kinetic energy supplied by the jet, L_j, and the jet thrust, T_j. In the classic case the jet velocity is given by: $v_j = L_j/T_j$ for high Mach jets (see Dreher 1985, Bridle and Perley 1984, and Williams 1991 for the relativistic generalization). The standard assumption is that $L_j = L_R/\epsilon$ where L_R = lobe radio luminosity = 4.4×10^{44} erg sec^{-1}, and ϵ is an efficiency factor for converting bulk kinetic energy into radio luminosity. The thrust can be estimated from: $T_j = P_{HS} \times A_{HS} = 4 \times 10^{35}$ ergs cm^{-1}, where P_{HS} = minimum energy hotspot pressure = 3×10^{-9} dyn cm^{-2}, A_{HS} = hotspot area = 1×10^{44} cm^2, leading to: $v_j = 0.04c/\epsilon$.

Estimating ϵ is difficult. It has been suggested that jet shocks are very efficient at converting bulk kinetic energy into relativistic particles (Axford, Leer, and McKenzie 1982, Bell 1987). At the minimum the jet must also do work to expand the ambient medium: work $\approx P_L \times V_L \approx 10^{59}$ ergs, where P_L = lobe pressure = 8×10^{-11} dyn cm^{-2}, and $V_L = 7 \times 10^{68}$ cm^3. Dividing this by the source lifetime of $t_s \approx 10^{6.8}$ yrs (as estimated from synchrotron spectral ageing arguments; see below) yields 5×10^{44} ergs sec^{-1}, thereby setting a very rough upper limit: $\epsilon \leq 0.4$. In reality, ϵ is likely to be considerably less than this (Dreher 1985, Leahy 1991), in particular if the lobe pressures are substantially different than dictated by minimum energy.

One can also consider the total mass flux in the jet and the upper limit to the mass in the radio lobes, M_L, to derive a jet velocity: $v_j = t_s \times P_{HS} \times A_{HS} / M_L$. Using a lobe density $< 2 \times 10^{-4}$ cm^{-3} derived from the lack of internal Faraday dispersion (Dreher et al. 1987) implies $M_L < 2.4 \times 10^{41}$ gm. The lower limit to the jet velocity is then $0.01c$.

Both of the above calculations are invalid in the case of departure from minimum energy conditions, or a time-variable energy (or mass) supply in the jet. The mass estimate also depends on the assumptions of magnetic field strength and geometry inherent in the internal Faraday depolarization calculation.

Williams (1991) develops a simple hydrodynamic model relating observable parameters such as the ratio of jet width to lobe width and the ratio of hotspot pressure to lobe pressure to physical parameters such as the jet Mach number and ambient-to-jet density contrast. Applying this model to Cygnus A he finds $M_j \approx 8$, and $\eta \approx 2 \times 10^{-4}$ for a Newtonian ideal fluid. He then balances jet ram pressure against minimum pres-

sures in the hotspots and finds a required jet velocity somewhat greater than the speed of light. Williams uses this result to argue that the jet must be relativistic on kpc-scales, and must be composed primarily of a relativistic (pair) plasma. However, his calculations apply to axisymmetric flows in a constant density medium. Including jets which vary direction on short timescales, and/or density gradients in the ambient medium, would widen the lobes over the axisymmetric case, and invalidate the above arguments.

Muxlow, Pelletier, and Roland (1988) and Carilli et al. (1991a) have used the observed spectra of the Cygnus A radio hotspots to constrain various physical parameters of the jet. Their basic conclusion is that the various 'features' in the hotspot spectra are consistent with a model involving particle acceleration at a strong shock in a Newtonian fluid with a mildly relativistic jet velocity ($\approx 0.4c$).

Roland and Hermsen (1995) develop a two-component model for the jets in extragalactic radio sources involving a narrow 'core' jet consisting of a pair-plasma, and moving at $\approx c$, sheathed by a classical (proton-electron) plasma moving transrelativistically ($\leq 0.7c$). The relativistic jet component gives rise to the large Lorentz factors, and γ ray emission, from superluminal radio jets, while the classical component dominates the dynamics, and gives rise to the large scale radio emitting structures (lobes, hotspots, etc...).

Overall, there are no data which necessitate a highly relativistic jet on kpc-scales or a jet consisting of only pair plasma (Begelman et al. 1984) in Cygnus A. On the other hand, neither of these is currently precluded, emphasizing our current ignorance of the real physical conditions in jets. Mildly relativistic flow would be consistent with the observed jet-to-counterjet surface brightness ratio, as discussed below.

The hotspots

Structure: the dentist's drill

Hotspots in radio galaxies were first discovered in the occultation experiments of Swarup, Thompson, and Bracewell (1963). Since then hotspots at the source extremities have been a defining characteristic of FRII radio galaxies.

The high resolution images of the hotspot regions in Cygnus A are shown in Fig. 7. There are two hotspots in each lobe, designated A and B in the northern lobe, and D and E in the southern lobe (Hargrave and Ryle 1974, Miley and Wade 1971). The presence of multiple hotspots, and in particular compact 'primary' hotspots (B and E, in the case of Cygnus A), and more diffuse 'secondary' hotspots (A and D), appears to be common in powerful radio galaxies (Lonsdale and Barthel 1986, Laing 1989), although more complex morphologies are also seen (Black et al. 1992).

Early models to explain multiple hotspots in powerful radio galaxies included complex shock structures in axisymmetric jets (Norman et al. 1982), and local instabilities along the contact-discontinuity (Kronberg et al. 1977). However, the generally accepted model today for multiple hotspots is the 'dentist drill' model, in which jets alter direction on time-scales shorter than the timescale it would take for an 'abandonned' hotspot to fade to the background surface brightness level due to expansion loses ($\approx 10^5$ yrs; Carilli et al. 1988). This model is consistent with a number of observations, including: lobes which are wider than expected from axisymmetric models, primary hotspots that are recessed from the ends of the radio lobes, and jets which

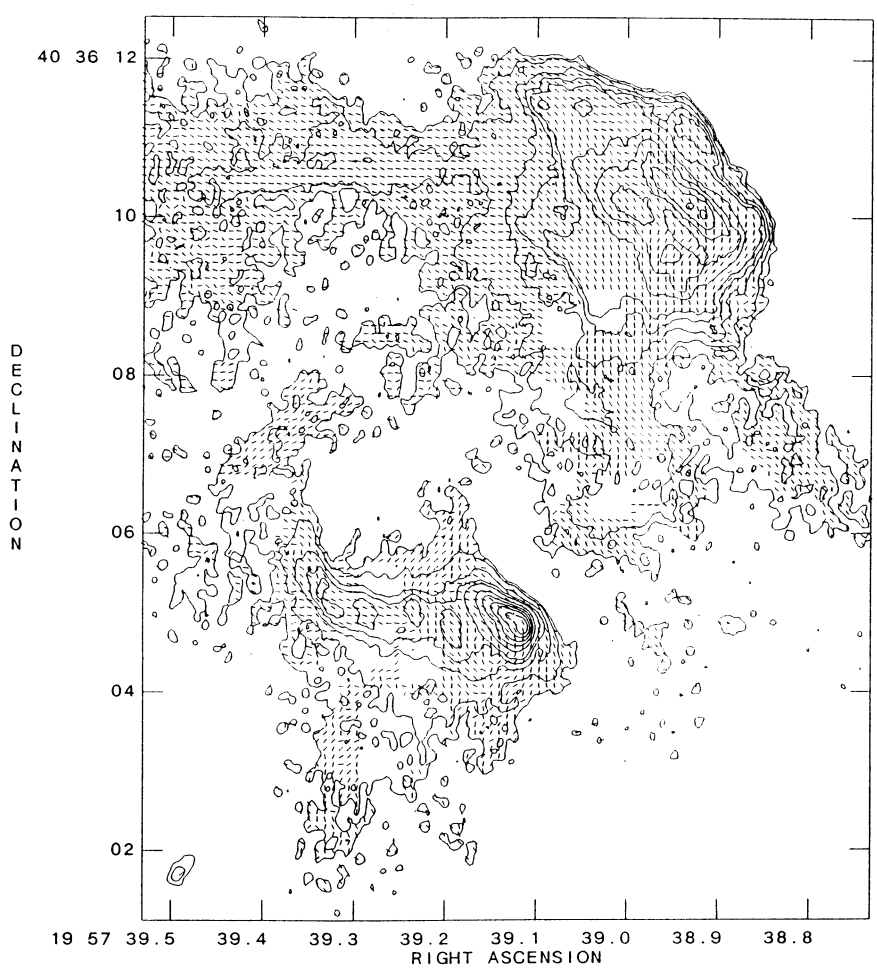

Fig. 7. The contours show the total intensity at 15 GHz, 0.1″ resolution of the northern (above) and southern (next page) hotspot regions in Cygnus A (reproduced from Carilli, Dreher, and Perley (1989a). The contour levels are 2, 3, 6, 9, 12, 21, 30, 39, 48, 57 mJy/beam for the northern hotspot, and 2, 2.8, 4, 5.6, 8, 11, 16, 22, 32, 45, 64, and 91 mJy/beam for the southern hotspot. The line segments denote the direction of the projected magnetic field, derived from the polarized emission, after correction for Faraday rotation. We follow the nomenclature of Hargrave and Ryle (1974), who designated the large and small hotspots in the northwest lobe as A and B, and D and E in the southeast lobe, repectively

are not always straight from the core to the hotspot (Williams and Gull 1985, Carilli et al. 1988, Williams 1991, Cox et al. 1991, Black et al. 1992). In this model the primary hotspot represents the newest hotspot where the jet impinges obliquely on the side wall of the radio lobe, extending and widening the lobe in this new direction.

The secondary hotspot could be explained by one of two models. First, the secondary may be powered by collimated outflow from the primary, i.e. the ‘splatter spot’ model (Williams and Gull 1985, Smith 1984). An argument in favor of this model in some sources is that the projected magnetic field in the primary hotspot points towards the secondary hotspot (Lonsdale and Barthel 1986). However, the

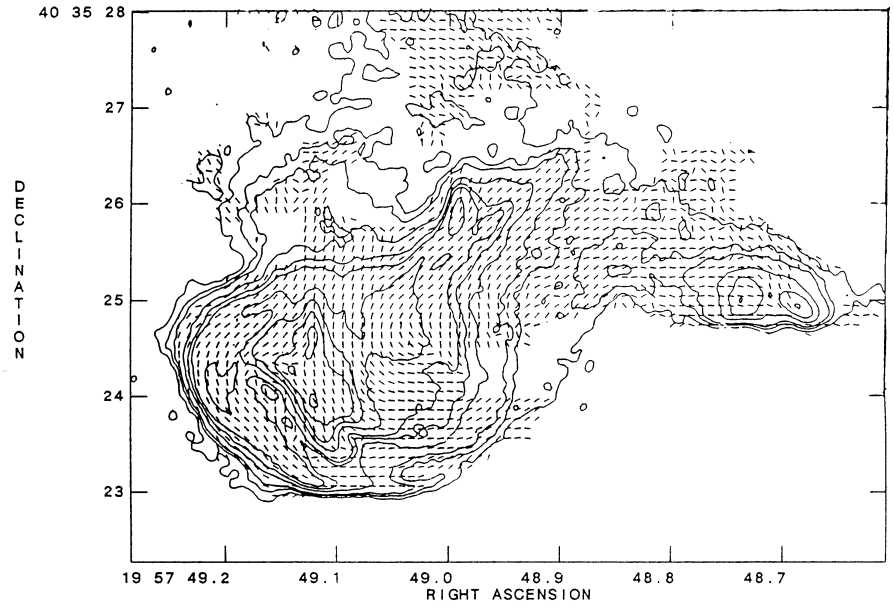

Fig. 7. (continued)

question remains: how to obtain such well collimated powerful outflow from the primary to the secondary, especially considering the large angles implied in sources like Cygnus A? One proposed solution is re-collimation of the post-shock primary hotspot fluid through a de Lavall nozzle (Lonsdale and Barthel 1986, Norman 1992), although the physical viability of such a solution has been called into question by a number of authors (Wilson 1989, Cox et al. 1991). This also leaves open the question: why is the total energy in the secondaries about an order of magnitude larger than in the primaries in most sources (Valtaoja 1984)?

An alternative model for powering the secondaries is to assume that the secondaries are the old hotspots, i.e. the location of previous jet termination. Besides the hotspot magnetic field structure already mentioned, the difficulties in this case are that the structure of the secondaries resembles that expected for a terminal Mach disk as discussed below, and that the spectra of the secondaries are consistent with current, or very recent, particle acceleration. A solution to these questions has been proposed by Cox et al. (1991) and Hardee and Norman (1990), in which the secondaries are still being fed by the remnant of the jet which has 'broken' along its course. The 3D simulations of Cox et al. (1991) are particularly relevant, in that they show transient, and complex, hotspot structures at various times during the lifetime of the source, consistent with the myriad structures seen in hotspot regions in many powerful radio galaxies (Black et al. 1992).

In this second case, the well-developed secondaries may then correspond roughly to terminal 'Mach disks' predicted for axisymmetric jets. The double-ridge structure seen at high surface brightness levels in both hotspots A and D in Cygnus A has been modeled in detail by Clarke et al. (1989). They predict similar double structure in the terminal Mach disk of a jet with a passive helical magnetic field, when the jet is oriented at a small, but finite angle with respect to the sky plane ($\approx 15°$). Of course,

the simulations by Clarke et al. (1989) were in 2D. More recent work suggests that terminal Mach disks tend to be very unstable when generalized to 3D, and that the more likely scenario for a jet terminus is a series of oblique shocks (Clarke priv. comm.). Dreher (1981) discusses hotspots in Cygnus A and other radio sources and demonstrates convincingly that elongated structures like the ridges in the Cygnus A hotspots are most-likely two-dimensional (disk-like), and not one-dimensional (rope-like).

A final point that is relevant in the interpretation of the shock structures at the jet terminus in Cygnus A is the bow shock discovered in the rotation measure distribution by Carilli et al. (1988). The bow shock preceding the primary hotspot B in the northern lobe was detected via its contribution to the rotation measure distribution in this region. The bow shock is seen as an 'arc' of discontinuous change in rotation measure (RM) roughly concentric with the primary hotspot, with a standoff distance of about $3''$. This jump in RM signals the point at which the thermal particles and tangential magnetic fields in the ICM are compressed by the shock due to the supersonic advance of the primary hotspot.

Detecting this radio quiet bow shock has a number of important implications on our understanding of source dynamics. First, it confirms the basic double-shock structure for the jet terminus in powerful radio galaxies and that the radio emission is contained within the contact discontinuity, at least in Cygnus A. Second, the fact that the bow shock projects onto the lobe dictates the three-dimensional geometry of the source such that the primary hotspot B lies along the near-side wall of the radio source.

The radio lobes

The bridge and plumes

At low frequency Cygnus A displays a 'radio bridge' connecting the high surface brightness regions at the source extremities (Fig. 10). Whether the radio bridge forms a physically connected structure through the center of the galaxy, or just appears to in projection, remains an open question. The comparison of radio and line emission in the center of the Cygnus A galaxy (Jackson et al. 1994, Carilli et al. 1989b) suggests that the lobes may not have completely evacuated the inner $\approx$ 10 kpc of the galaxy.

At the center of the bridge are seen 'plumes' of emission extending to the north and south. Leahy and Williams (1984) and Williams (1985) present a detailed analysis of radio bridges and bridges distortions in powerful radio galaxies, including Cygnus A. The plumes in Cygnus A are most consistent with Williams' model A in which back-flow of radio emitting fluid in the lobe is deflected away from the high pressure central regions of the galaxy by the general pressure gradient in the ICM.

The filaments

Filamentary structure in the radio lobes of Cygnus A was discovered in the high dynamic range VLA images by Perley et al. (1984). Since then filamentary structure has been seen in most extragalactic radio sources observed with sufficient sensitivity

and resolution (Hines et al. 1990, Fomalont et al. 1989, Dreher and Feigelson 1984, Clarke et al. 1992).

An important question raised when filamentary structure was first observed in radio galaxies was whether the volume filling factor for radio emitting fluid in the lobes could be very low. Perley et al. (1984) estimate that the volume filling for the lobes of Cygnus A could be between 0.03 and 0.3. On the other hand, detailed analysis of surface brightness profiles of the lobes shows that there is a space filling diffuse component (Carilli 1989, Leahy 1991). Although noticeable to the eye, the surface brightness contrast between the filaments and the background is typically $\leq$ 20% at 4.5 GHz, with a few filaments contrasting by up to 50%. If the filaments are rope-like (one-dimensional) their minimum pressures are typically about a factor four larger than their environments, while if they are sheet-like (two-dimensional) they are only over-pressured by 30% or so.

Many explanations have been considered for filaments in radio sources, including cooling instabilities (Eilek 1989), regions of anomalous resistive reconnection (Eilek 1989, Hines et al. 1990, Christiansen 1989), turbulent vortices in back-flow in the radio lobe (Norman et al. 1982), and weak shocks, or non-linear (Mach 1) acoustic waves driven by the pressure difference between the hotspots and lobes (Carilli 1989).

The most recent and convincing explanation of filamentary structure in radio galaxies is that coming from the 3D simulations of Clarke (1992) which include passive magnetic fields. He finds the natural development of rope-like filaments in radio lobes corresponding to regions of enhanced, or 'bundled' magnetic field. Importantly, he notes no evidence for enhanced thermal densities or pressures in these regions. The intermittent bundles of enhanced field occur in regions of large velocity shear implying a simple kinematic dynamo process as the origin for the enhanced (although still dynamically weak) field regions. The polarization characteristics of these filaments are consistent with that observed for Cygnus A (high fractional polarization with longitudinal fields).

A possible physical diagnostic for filamentary structure in radio lobes is the power spectrum. Carilli (1989) measured a power-law power spectrum of the form: P(k) $\propto$ $k^{-2.6}$, on spatial scales (= 1/k) between 0.7″ and 8″. Eilek (1989) shows that an observed power-spectrum of index ≈ -3 might result from isotropic, weak-field Kolmogorov turbulence.

DeGraff (1992) has performed a fractal analysis of the filaments in Cygnus A. He obtains a fractal dimension between 0.4 and 1.2, consistent with the elongated appearance of the structures. DeGraff and Christiansen (1996) show that the fractal spectra of the filamentary structure in the lobes of Cygnus A are best reproduced with turbulent models involving spatial variations in both the fields and the relativistic particles.

Radio continuum spectroscopy

Synchrotron spectral ageing

Mitton and Ryle (1969) first noted that the radio spectral index flattened towards the extremities of the radio source in Cygnus A. This flattening was confirmed in the images of Hargrave and Ryle (1974), who showed that the radio hotspots had the flattest spectra in the source (besides the core). This effect can be seen in the

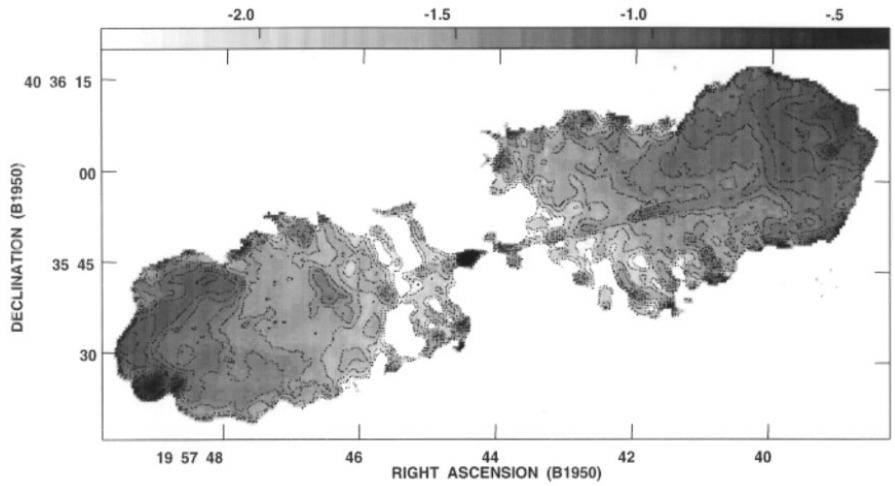

Fig. 8. The spectral index distribution across Cygnus A between 1.5 GHz and 5 GHz at $1.1''$ resolution. The grey-scale ranges from -2.4 (white) to -0.4 (black), and the contour levels are: -2.5, -2.3, -1.9, -1.7, -1.5, -1.4, -1.3, -1.2, -1.1, -1.0, -0.9, -0.8, -0.7, -0.5

spectral index image of Cygnus A in Fig. 8. The hotspots have spectral indices of -0.5 between 1.5 GHz and 5 GHz, with gradual steepening of the spectra to indices ≤ -2 in the tails of the radio lobes.

The spectral steepening seen in Cygnus A is characteristic of powerful radio galaxies in general. This effect has been explained as synchrotron radiative ageing of the relativistic electrons. Synchrotron radiation preferentially depletes the highest energy electrons, leading to a steepening in the emission spectrum at high frequencies over time (Pacholcyzk 1970, Scheuer and Williams 1968). A synchrotron-aged radio spectrum is characterized by an (assumed) low frequency power-law emission spectrum of index $\alpha_{\rm in}$, a 'break frequency', $\nu_{\rm B}$, near which the spectrum steepens from the injected power-law, and the behavior above the break, which depends on microphysical processes such as pitch angle scattering and particle acceleration (Myers and Spangler 1985, Carilli et al. 1991a). The 'injection index', $\alpha_{\rm in}$, relates to the energy index for the relativistic electron population, $S_{\rm in}$, as: $S_{\rm in} = 2\alpha_{\rm in} - 1$, where $N(E) \propto E^S$ (Pacholcyzk 1970). The radiative 'age' of the relativistic particle distribution, $t_{\rm syn}$, defined as the time since the spectrum was a power-law out to infinite frequency, relates to $\nu_{\rm B}$ and the magnetic field, B, through: $t_{\rm syn} = 1610 B^{-3/2} \nu_{\rm B}^{-1/2}$ Myr, with B in μG, and $\nu_{\rm B}$ in GHz [2].

The inference is that the electrons at the center of the source are 'older' than those closer to the hotspots, i.e. that the source is expanding in time with the principal site of particle acceleration being the hotspots, in agreement with the jet model. The connection between radio spectrum and age allows for a study of the growth and evolution of the lobes by careful measurement of the spectrum throughout the length and width of the source. Extensive synchrotron 'spectral ageing' studies of radio

[2] Inverse Compton losses have been ignored. For Cygnus A the energy density in the ambient photon field is $\leq 1\%$ that in minimum energy magnetic fields throughout the source. Note that in general this may not be true, in particular for low surface brightness sources, and/or for sources at high redshift, where the microwave background energy density can become substantial.

galaxies have been performed by many authors (Burch 1979, Alexander 1985, 1987, Alexander and Leahy 1987, Myers and Spangler 1985, Leahy, Muxlow, and Stevens 1989). Using minimum energy magnetic fields these studies have led to lifetimes for powerful radio galaxies between 10^6 and 10^8 yrs, and advance speeds between 0.02 and $0.2c$. The validity of spectral ageing analyses is supported by the general agreement between spectral ages and upper limits to source lifetimes dictated by the space density of powerful radio galaxies ($\leq 10^8$ yrs; Schmidt 1965), and upper limits to source expansion velocities set by special relativity and the statistics of arm-length asymmetries for lobes in radio galaxies ($\leq$ 0.2c; Longair and Riley 1979).

Spectral ageing studies also allow for the study of the micro-physical processes in the relativistic electrons by determining the behavior of the spectrum at frequencies higher than the break frequency (Kardashev 1962, Pacholcyzk 1970, Jaffe and Perola 1973, Eilek and Shore 1989, Carilli et al. 1991a).

Cygnus A has been the most exhaustively studied of all radio galaxies in this regard (Winter et al. 1980, Alexander et al. 1984, Roland et al. 1988, Muxlow et al. 1988, Carilli et al. 1991a). The difficulty in spectral ageing studies of radio galaxies is that the curvature in the spectrum is very gradual, requiring sensitive observations to be made over a large frequency range at matched spatial resolution. The large angular size and high flux density of Cygnus A over a wide range in frequency has allowed for the first fundamental test of synchrotron radiation theory, and we review the results herein.

The hotspot spectra

The integrated spectra of the hotspots in Cygnus A at $4.5''$ resolution are shown in Muxlow et al. (1988) and Carilli et al. (1991a), while high resolution ($0.4''$) spectral index images can be found in Carilli et al. (1989a) and Perley and Carilli (1996). The integrated spectra above 1 GHz are well fit by a continuous injection (CI) model spectrum, in which a power-law distribution of particles is continuously injected at the hotspot. The injection index is -0.5 ± 0.1 for both hotspots – typical for hotspots in high power radio galaxies (Meisenheimer et al. 1989). Diffusive shock acceleration theory predicts: $\alpha_{\rm in} = 3/(2-2r)$, where r is the shock compression ratio (Bell 1978a,b, Blandford and Ostriker 1978). For a strong shock in a monatomic Newtonian fluid, $r = 4$, and hence $\alpha_{\rm in} = -0.5$. However, the effects on injection index assuming a relativistic jet velocity, or allowing for modification of shock structure due to up-streaming high energy particles, are minor, $\pm$ 0.1 or so in spectral index, and certainly cannot be ruled out (Kirk and Schneider 1987, Drury and Völk 1981, Axford et al. 1982, Kirk 1989, Heavens 1989, Eilek and Hughes 1991).

The two dominant hotspots in Cygnus A (denoted A and D in Hargrave and Ryle 1974) have break frequencies around 10 GHz, implying spectral ages $\approx 10^5$ yrs using minimum energy fields. Above the break the spectra are consistent with a power-law of index -1.0 out to at least 375 GHz. The hotspots have not been detected in the optical (Kronberg et al. 1977, Röser 1996). The optical upper limits fall two orders of magnitude below the extrapolation of the power-law from 375 GHz into the optical, suggesting a sharp cut-off in the spectra between 375 GHz and 10^{14} Hz (Harris et al. 1994a, Röser 1996).

The physical interpretation of spectral breaks in hotspot spectra is discussed at length in Muxlow et al. (1988), Roland et al. (1988), Meisenheimer et al. (1989),

and Carilli et al. (1991a). The basic model involves relativistic particle injection at a 'point', i.e., the terminal jet shock, and then convection away from the high field post-shock regions with the general outflow. The isotropic outflow velocity, v_{out}, is given simply by the radius of the high surface brightness hotspot region (or the beam size, if it is smaller) divided by the spectral age derived from the hotspot spectrum. For Cygnus A the value for both hotspots is: $v_{out} \approx 0.06c\ h^{-1}$. For a strong shock the inflow velocity is four times the outflow velocity (in the shock frame) implying an inflow velocity of $0.24c\ h^{-1}$. Carilli et al. (1991a) discuss the possible effects an anisotropic outflow may have on the above analysis.

The Cygnus A hotspot spectra continue to flatten below 1.5 GHz. Muxlow et al. (1988), Leahy et al. (1989), and Carilli et al. (1991a), have all argued that the low frequency flattening of the hotspot spectra in Cygnus A is due to a low energy cut-off in the relativistic electron population at Lorentz factors of ≈ 450 (assuming minimum energy magnetic fields). Such a cut-off was predicted by Bell (1978) in his original work on shock acceleration. Bell hypothesized that in order for a particle to be 'injected into the acceleration process' it must have sufficient momentum to pass unperturbed through the potentials in the collisionless shock which act to stop the jet. In essence the relativistic electrons must have gyro-radii which are larger than the shock width, which in a collisionless shock is of order the gyro-radius of the thermal protons (see also Eilek and Hughes 1991). The alternative explanation of synchrotron self-absorption leads to fields strengths that are many orders of magnitude above equipartition values, while thermal absorption implies local densities inconsistent with redshifted Hα imaging of Cygnus A.

Lobe spectra and the age of the radio source

Spectral ageing across the radio lobes has been considered in detail by Alexander et al. (1984, 1996) and Carilli et al. (1991a). These studies find a roughly linear increase in age with distance from the hotspots. The implied 'separation velocity' is $0.045c\ h^{-1}$, derived using minimum energy fields of 50μG. The oldest electron populations are found in the radio 'plumes' extending to the north and south of the center of the radio bridge, with an implied source age of 6 Myr.

As pointed out by Winter et al. (1980) the separation velocity measured from spectral ageing is the sum of two velocities: the source advance speed and the back-flow velocity of material in the lobes. An important question is whether the waste hotspot material is simply left behind by the advancing lobes (back-flow velocity = 0), or whether there is bulk fluid flow back towards the galaxy? An independent estimate of the advance speed comes from the ram pressure calculation. The ram pressure advance speed for the hotspots in Cygnus A is $0.02c$, derived using minimum energy fields. In the context of the dentist's drill model Williams (1985) has shown that for sources in which the hotspots cover only a small fraction of the heads of the source such as Cygnus A the overall ram pressure advance speed must be lowered by the ratio of the hotspot area to the area of the heads of the lobes. In Cygnus A this would decrease the advance speed by another order of magnitude. This leads to the problem that the source advance speed derived from ram pressure arguments is well below the separation velocity derived from spectral ageing analysis. A back-flow velocity $>>$ source advance speed contradicts very basic continuity arguments in Cygnus A for which the radio plumes (presumably the catch-basin for the back-flow) constitute only

a small fraction of the total volume of the source (Carilli et al. 1991a). This problem is alleviated by considering that the source may still be expanding transversely, and aggravated by the possibility that the source advance may have been slower in the past due to the overall density gradient in the cluster (Arnaud et al. 1984). A possible solution is to allow departures from minimum energy conditions. Carilli et al. find a self-consistent, although admittedly ad hoc, model is possible in which the the fields are systematically below minimum energy by a factor of three resulting in an average source advance speed $\approx$ separation velocity $\approx 0.01c$, and a source age of 30 Myr.

Alexander et al. (1984, 1996) and Carilli et al. (1991a) argue that expansion losses are large going from the hotspots to the radio lobes but that in the lobes themselves the dominant energy loss mechanism is synchrotron radiation. In terms of the shape of the spectra above the break Carilli et al. find that the lobe spectra steepen more than allowed by continuous injection models, but less steeply than exponential. The best fitting model involves 'one-shot' injection with subsequent radiative losses, but without continuous isotropization of the pitch-angle distribution which would lead to an exponential cut-off (Pacholcyzk 1970, Jaffe and Perola 1973, Kardashev 1962).

Overall, the general evolution of spectral steepening with distance from the hotspots, and the fact that the lobe spectra steepen more than allowed in the case of continuous injection, are in good agreement with synchrotron spectral ageing theory and the jet model for powerful radio galaxies. However, there are a few difficulties with this simple analysis. First are the difficulties encountered when considering the relative contribution of back-flow and source advance to the separation velocity as derived under minimum energy conditions, as discussed above. Second, Carilli et al. determine an injection index of -0.7 in the radio lobes, while the best fit value for the hotspots is -0.5. This 'injection index discrepancy' is difficult to reconcile with the idea that the principal location of particle acceleration is the hotspot[3]. And third, the lack of an exponential cut-off implies no pitch angle scattering of the relativistic particles. This is hard to justify physically since pitch angle scattering of streaming electrons by self-induced Alfven waves is thought to be an efficient process (Eilek and Hughes 1991, Wentzel 1974, Wentzel 1969).

Another important question in spectral ageing analyses is the possibility of a temporally and/or spatially variable magnetic field and their effect on derived synchrotron ages. This question has been considered by a number of authors (Wiita and Gopal-Krishna 1990, Siah and Wiita 1990, Tribble 1993). Tribble shows that allowing for a distribution of magnetic field strength requires the use of a weighted-mean field strength in the age calculation. He also shows that a distribution in field strength solves the exponential cut-off problem (or lack thereof), by 'smearing-out' the individual exponentially steepening spectra resulting in observed spectra similar to those found in the lobes of Cygnus A.

[3] An interesting aside is the fact that a similar 'injection index discrepancy' exists for cosmic rays in the disks of spiral galaxies. The observed index for the integrated emission from spiral galaxies is typically -0.7, while the average supernova remnant (presumably the sites of cosmic ray acceleration) has an index of -0.5 (Condon 1992). The solution proposed in the case of spiral galaxies is energy dependent cosmic ray diffusion. However, this solution cannot be invoked in the case of radio galaxies, since diffusion is probably insignificant compared with convection for relativistic electron transport in the lobes (Carilli et al. 1991a).

An alternative: the universal spectrum

The basic premises of spectral ageing analyses of the type discussed above have been called into question recently by Rudnick and Katz-Stone (1996), Rudnick, Katz-Stone, and Anderson (1994), Katz-Stone and Rudnick (1994), and Katz-Stone, Rudnick, and Anderson (1993). They re-analyze the spectral data for Cygnus A and reach some disconcerting conclusions. First, they question the existence of a power-law in any region of the spectrum. And second, they find that all spectra in the source, hotspots and lobes alike, can be explained by simply shifting (in the log plane) a single continuous function. They argue for a 'universal spectrum', with 'no evidence for evolution of the electron energy distribution', other than this simple scaling in frequency and/or intensity.

They reach these conclusions through the use of a radio 'color-color' diagram. The radio color-color diagram entails plotting for each position in the source the observed spectral index between two frequencies against that between two other frequencies. They point out that such two-color diagrams have a few advantages over multi-frequency spectral model fitting, including: emphasizing more clearly curvature in spectra and 'displaying information from all positions in a source in a way that enables one to see the real connections between the various spectra'. Most importantly, their approach is strictly empirical, and hence may reveal trends in the data which are missed in an analysis fundamentally tied to a physical model.

The color-color diagram for Cygnus A reveals a well-defined locus of points. This locus can be described empirically by a single spectral shape (the 'universal spectrum') through simple scalings in frequency and/or intensity. As further proof Rudnick et al. have taken spectra from three different regions of Cygnus A (hotspots and lobes included) and scaled each accordingly to fit this universal spectrum.

Katz-Stone et al. (1994) have shown that given a spectral index image, an image of total intensity, and the empirically derived universal spectrum, one can derive images based on products of pairs of three basic physical parameters: the magnetic field strength, the relativistic particle density, and the 'characteristic energy' for the particle distributions. They apply this 'color-correction' technique to Cygnus A and find that the eastern lobe shows a bright 'channel which straddles the counterjet.' They suggest that this channel is dominated by a density enhancement, rather than by magnetic or energy effects.

The fundamental appeal of the two-color analysis is its independence from physical assumptions. The ultimate goal of relating the results to fundamental source physics remains under investation (Rudnick and Katz-Stone 1996). One particular question that must be addressed is: how to avoid the inevitable effects of synchrotron losses on the emitted spectra? Also, the fact remains that in terms of a proper χ^2 fitting with well defined errors, spectral ageing theory cannot be precluded by the data (Carilli et al. 1991a).

Overall, the numerous spectral studies of Cygnus A have emphasized the fundamental difficulty in quantitative analysis of radio continuum spectra, namely, the extremely broad range in frequency required to constrain the various models. Further insight into the validity of spectral ageing theory, or a universal spectrum, requires either arcsecond resolution imaging at very low frequency ($\leq$ 100 MHz), or extremely sensitive observations at high frequency, both of which are at the limit of current instrumentation.

Magnetic fields

Minimum energy

A fundamental parameter in the physical analysis of radio galaxies is the magnetic field strength. Most studies of cosmic radio sources use the 'minimum energy' assumption to estimate field strengths. The minimum energy calculation, first presented by Burbidge (1956), relies on the fact that given a synchrotron emissivity, the summed energy density in relativistic particles and magnetic fields can be minimized by adjusting the magnetic field strength. The minimum energy condition implies rough equipartition of energy between fields and relativistic particles. Whether such a minimum configuration for the fields and particles is reached remains to be verified (Leahy 1991).

The minimum energy calculation involves a number of assumptions, as outlined in Miley (1980). The values for minimum energy fields quoted herein are calculated from Miley's equation 2, with unity filling factor, and lower and upper cut-off frequencies of 10 MHz and 100 GHz, respectively. The most important unknown parameter in this calculation is the 'k factor', where k is the ratio of energy density in relativistic protons to that in relativistic electrons. We use a value of k = 1, unless stated otherwise. We also assume fields which are tangled on scales much smaller than our resolution element [4]. Such a field configuration implies that the effective magnetic pressure (including the tension term) is 1/3 times the magnetic energy density. In this case the total pressure in relativistic particles and fields is simply 1/3 times the total energy density, and minimizing total pressure yields the same result for both fields and pressures as minimizing total energy density (Leahy 1991). We also use h = 0.75 for deriving the minimum energy fields, since the fields are insensitive to h (fields $\propto$ $h^{2/7}$).

For the hotspots in Cygnus A we calculate fields from the observed surface brightness distribution at 15 GHz at $0.1''$ resolution, assuming a disk-like geometry and a spectral index of -0.5. Minimum energy fields vary from 250 μG to 350 μG on the high surface brightness structures. We use a value of 300 μG as representative, with the corresponding minimum pressure of 3×10^{-9} dyn cm^{-2}. For the lobes we calculate minimum energy fields from the observed surface brightnesses on the 327 MHz image at $4.5''$ resolution, assuming a cylindrical geometry with a width of $25''$ and a spectral index of -0.7. Fields vary from about 65 μG in the heads of the lobes to 45μG in the center of the radio bridge. Corresponding pressures are 1×10^{-10} dyn cm^{-2} and 6×10^{-11} dyn cm^{-2}, respectively. For the kpc-scale radio jet we assume a spectral index of -0.8 and a cylindrical geometry with a width of $1''$. The fields in the jet knots are about 130μG, and the corresponding pressure is 6×10^{-10} dyn cm^{-2}.

[4] Maxwell's equations, in particular a divergence-less field, prohibit a truly isotropic microscopic field distribution. When we discuss tangled fields, we mean tangled on scales less than the resolution element.

Fractional polarization and projected field morphology

Multi-frequency radio continuum polarimetric imaging determines both the fraction of the total intensity which is linear polarized at a given frequency, and after a proper correction has been made for Faraday rotation as discussed below, the projected magnetic field structure in the radio source. The theoretical maximum fractional polarization, FP, for optically thin synchrotron emission from a population of relativistic electrons with a power-law energy distribution and an isotropic pitch angle distribution in a uniform magnetic field is: FP = $(1-\alpha)/(5/3-\alpha)$, or 72% for $\alpha = -0.7$ (Pacholcyzk 1970). Fractional polarizations are high in Cygnus A, with typical values between 10% and 40%, and reaching as high as 70% in the jet and hotspots at high resolution (Carilli et al. 1989a).

The projected magnetic field distribution across the radio lobes is shown in figure 9. The projected fields generally follow parallel to the edges of the source, to the bright ridges in the hotspots, to the filamentary structure in the lobes, and along the jet.

Laing (1980) presents an analytic model for magnetic fields in radio galaxies which explains very nicely the observed fractional polarization and projected field structure in Cygnus A. His model involves simple kinematic dynamo processes in the radio source, i.e. shear and/or compression by turbulent fluid motions of a magnetic field which is 'frozen-in' to the fluid due to the very high conductivity of a collisionless plasma. Compression and shear can result in the creation of 'Laing cells' from a fully tangled initial field distribution. Such cells correspond to regions of highly anisotropically tangled field where one dimension of the turbulence is 're-organized' by compression or shear. In certain projections this can result in observed fractional polarizations approaching the theoretical maximum. The simple analytic model of Laing has been verified by 3D hydrodynamic simulations of radio jets with passive magnetic fields, including the field morphology in the jets, hotspots, and filamentary structure in the lobes (Clarke 1992, Mathews and Scheuer 1991, Cox et al. 1991).

Perley and Carilli (1996) present polarization images of Cygnus A at 8 GHz, 0.4″ resolution. They find very high fractional polarizations in the radio lobes, approaching 70% in some areas, and projected fields which follow parallel to the axis of the radio lobes. The implication is a very well ordered field in the lobes with the dominant field component projecting along the long axis of the lobe, as expected for example if the field is stretched by shear flow down the lobes. This suggests that the fluid dynamics in the lobes is not magnetically dominated (Blandford 1996).

The Faraday screen: magnetic fields in cluster gas

Slysh (1966) and Mitton (1971) first pointed out the 'anomalous' behavior of the polarized emission from Cygnus A, including changing fractional polarization with observed wavelength (at low resolution), essentially random projected electric field vectors, and a large difference between the magnitude of Faraday rotation measure (RM) towards the two lobes. This problem was delineated in detail in the study of the rotation measure distribution towards Cygnus A by Alexander et al. (1984). They find that the 'rotation measure values are very noisy, and no overall pattern can be discerned.' They suggest a Galactic origin for the rotation measures, based simply on the fact that Cygnus A has a fairly low Galactic latitude (b = 5.8°).

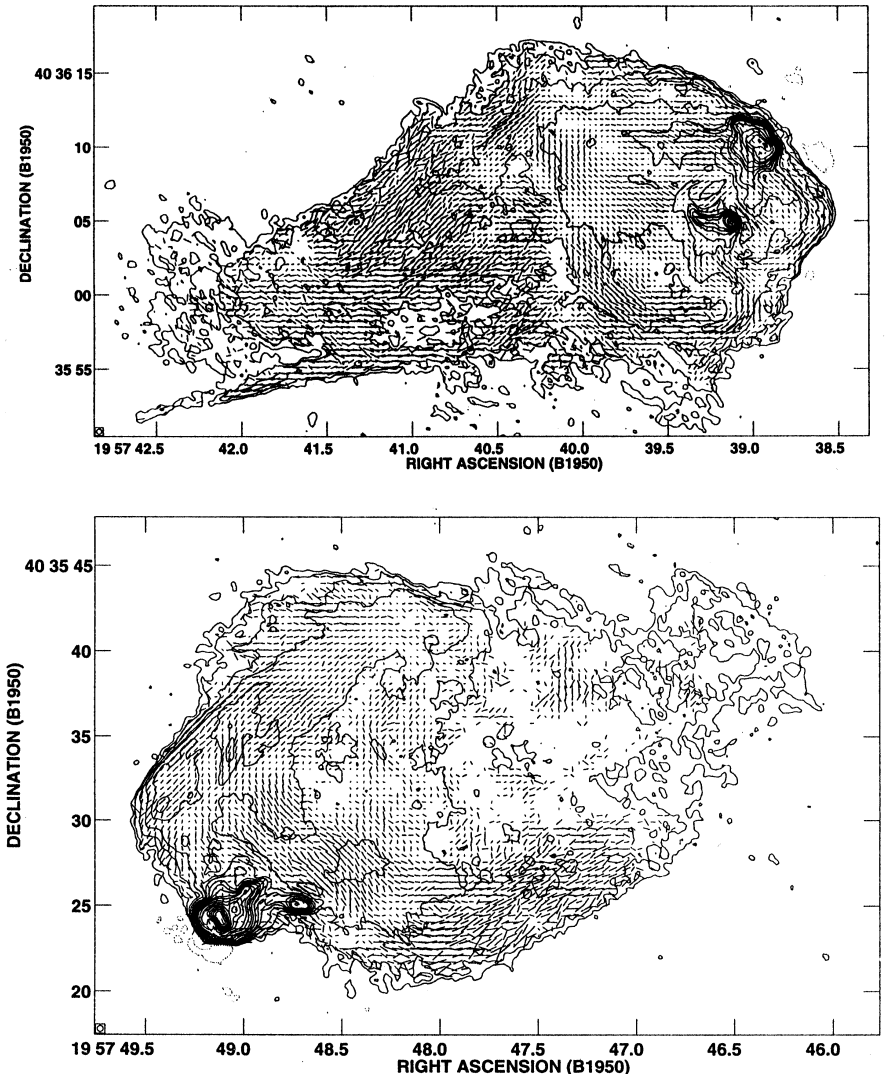

Fig. 9. The contours are of total intensity from Cygnus A at 8 GHz, 0.35″ resolution. The vectors show the projected magnetic field distribution across the source derived from the polarized emission after correction for Faraday rotation, reproduced from Perley and Carilli (1996)

The question of the large anomalous Faraday rotation towards Cygnus A was resolved by the sensitive, multi-frequency, spatially resolving polarization observations of Dreher et al. (1987b). These authors find that Cygnus A lies behind a deep 'Faraday screen', with rotation measures varying from -4000 rad m^{-2} to +3000 rad m^{-2} across the source. Gradients in RM exceed 300 rad m^{-2} arcsec^{-1} . In general the distribution is not random, but displays structure with coherence over spatial scales of order 10 kpc. Perhaps most importantly, Dreher et al. (1987b) find that the total rotation of the position angle of the polarization vector exceeds 600° in many regions,

without departure from a λ^2 dependence, where λ = observed wavelength, and without depolarization demonstrating conclusively that the Faraday rotation cannot be internal to the source but must be by an external screen (Burn 1966). This conclusion has been further strengthened by the recent 8 GHz results of Perley and Carilli (1996). The 8 GHz data set severe limits on deviations from a λ^2 dependence of position angle throughout the observed wavelength range.

Dreher et al. (1987b) consider, and reject, a Galactic origin for the Faraday screen. They propose that the origin of the large RM's is in the hot intracluster gas in which Cygnus A is embedded. The implication is that the large-scale cluster gas is substantially magnetized. Using the cluster gas density radial profile derived from X-ray observations, Dreher et al. calculate cluster magnetic field strengths between 2 μG and 10 μG, depending on geometry. Also, from the lack of wavelength dependent fractional polarization at fixed resolution, Dreher et al. derive an upper limit to the thermal electron density in the radio lobes of 2×10^{-4} cm^{-3}. This density limit depends on the minimum energy assumption for the radio source fields and assumes a uni-directional field through the lobes. Any field reversals along the line of sight would lead to a less stringent electron density limit.

An alternative model for the large rotation measures towards Cygnus A has been proposed by Bicknell et al. (1990), in which a thin mixing-layer exists along the contact discontinuity, where shocked cluster gas mixes with the large fields in the radio source. Support for this idea comes from the 'striated' appearance of the RM distribution across the radio lobes, suggestive of large-scale K-H instabilities at the contact discontinuity. However, since the discovery of extreme rotation measures towards Cygnus A spatially resolving observations of many radio galaxies at the centers of dense, X-ray emitting cluster atmospheres have revealed large rotation measures (for a summary, see Taylor et al. 1994). Taylor et al. show a clear correlation between the cluster core thermal density and the magnitude of RM's observed to cluster center radio sources. This includes both luminous edge-brightened (FRII) sources, such as 3C 295 (Perley and Taylor 1991), and less luminous edge-darkened (FRI) sources, such as M 87 (Owen 1989). Given that the physical interaction between the source and its environment is thought to be very different for the two types of sources (De Young 1993), we conclude that the majority of the large RM's observed must be the result of substantially magnetized, large scale cluster gas, and not simply the result of the interaction between the source with its environments.

The discovery of the bow shock in the RM distribution in the northern hotspot region in Cygnus A has relevance to this debate. Carilli et al. (1988) show that the observed RM change at the bow shock implies pre-shock intracluster fields of 8 μG. They propose a simple model in which the large-scale RM distribution towards Cygnus A (amplitudes up to 4000 rad m^{-2}, typical scale-sizes $\approx$ 10 kpc) is caused by the unperturbed cluster atmosphere, while small scale fluctuations (amplitude $\leq$ 1000 rad m^{-2}, scale-sizes $\leq$ 5 kpc) can result from the interaction of the source and the ambient medium.

In summary, the detection of extreme rotation measures towards Cygnus A, and subsequently in other cluster-center radio galaxies, shows that the thermal cluster atmospheres must be substantially magnetized, with fields $\geq$ a few μG. In most cases the pressure in the intracluster fields is below the thermal energy density (e.g. the plasma β-factor = ratio of thermal to magnetic pressure is between 20 and 50 for the Cygnus A cluster), implying a minor dynamical role for the fields. Even dynamically unimportant fields alter substantially the thermal conductivity of the plasma, and hence

are very important when considering the cooling and heating of the ICM (Sarazin 1986, 1988). Lastly, the detailed study of the Faraday screen towards Cygnus A provides vital supporting evidence for physical models explaining the depolarization asymmetries towards extragalactic radio sources and their implication for quasar-powerful radio galaxy unification schemes (Laing 1988, Garrington et al. 1988, 1991).

Models for the origin of intracluster fields include: the dynamo action of turbulent wakes of galaxies, injection of fields by previous outbursts of the radio source, ram pressure stripping of fields from galaxies, and amplification of a primordial field (Jaffe 1980, Ruzmaikin et al. 1989, Jafelice and Opher 1992; see Sarazin 1986, 1988 for reviews). Another possible mechanism for generating large scale cluster fields is amplification of seed fields during the merger of two clusters. Eilek (1994) presents a detailed 'Zeldovich rope dynamo' model for field generation in a cluster with net-helical turbulence, presumably driven by galaxy motions. She finds that the fields eventually evolve to equipartition strengths. She predicts RM distributions towards cluster center sources which compare well with observations, both in amplitude and structure.

The X-ray cluster

Large scale gas distribution

Cygnus A was first detected as an X-ray source by Giacconi et al. (1972) using the Uhuru satellite (see also Longair and Willmore 1974). Follow-up observations with the HEAO1 satellite by Fabianno et al. (1979) found that the source is spatially extended. They suggested that the emission is due to an atmosphere of hot gas with a temperature of 7×10^7 K, such as had been seen for the Virgo and Perseus clusters (see also Brinkman et al. 1977). This interpretation of a hot cluster halo for Cygnus A was confirmed by Arnaud et al. (1984) using the Einstein observatory. Their IPC image shows a very extended cluster gas distribution, with a radius $\geq$ 500 h^{-1} kpc, a density distribution $\propto$ radius^{-1}, and a total mass of 10^{14} $M_\odot$, while the Einstein HRI image revealed a dense core of emission, within which the radio source is embedded. The most recent treatment of the Cygnus A cluster gas emission is by Reynolds and Fabian (1996). Using ROSAT PSPC and HRI data, they show that the cooling time for the gas within $\approx$ 90 h^{-1} kpc is less than the Hubble time. They calculate a 'cooling flow' rate of $\approx$ 250 $M_\odot$ yr^{-1} for the dense cluster gas.

Spectral observations of Cygnus A with the Ginga satellite have refined the parameters for the cluster gas (Ueno et al. 1994). They find the total emission from Cygnus A is best fit by a two-component model including roughly comparable contributions from a highly absorbed power-law component (presumably the active nucleus), and from thermal cluster gas at T = 8.5×10^7 K. The absorption corrected luminosity of the cluster between 2 keV and 10 keV is 6×10^{44} h^{-2} ergs sec^{-1} (using a Galactic HI column density of 2.4×10^{21} cm^{-2}). They also detect iron line emission at rest-frame energy 6.9 keV, with a best-fit abundance of $\approx 0.3\times$solar. These conclusions have been confirmed through recent observations with ASCA (Arnaud et al. 1996). Lastly, the spatially resolving ROSAT PSPC observations of Cygnus A by Reynolds and Fabian (1996) suggest a temperature gradient to the cluster center, with the temperature decreasing from 8×10^7 K at radii $\geq$ 150 h^{-1} kpc, to 3×10^7 K in

the inner 50 h^{-1} kpc. Such a temperature decrease is qualitatively consistent with the cooling flow scenario.

The origin and evolution of hot cluster atmospheres is reviewed in detail in Sarazin (1986, 1988), and we refer the reader to these reviews for further details on this subject. We simply point out a few of the curiosities of the Cygnus A cluster. First is the anisotropic distribution of the cluster gas on large-scales. The cluster shows a long 'tail' extending about 500 h^{-1} kpc to the northwest. Such a morphology implies that the system has not reached final dynamical equilibrium, perhaps indicating a recent cluster merger (time-scale $\leq$ cluster sound crossing time $\approx$ 500 Myr). And second is that optical imaging of Cygnus A suggests that the Cygnus A cluster is poor in galaxies, with only four galaxies identified other than Cygnus A itself (Spinrad and Stauffer 1982). This contrasts sharply with the rich gaseous environment of the Cygnus A cluster, and leads to questions concerning the origin and heating of the cluster gas. However, the Cygnus A optical field is very confused, and images with sub-arcsecond resolution are required for proper determination of the true galaxy content of the Cygnus A cluster.

The second dynamical component

The unique aspect of Cygnus A is that it provides the opportunity to study the interaction between the radio source and the ICM in much greater detail than for any other powerful radio galaxy. Until now our understanding of the overall dynamics of powerful radio sources embedded in dense cluster atmospheres has been based strictly on radio observations. The advent of the sensitive, high resolution imaging capability of the ROSAT has finally revealed clearly the long hypothesized effects of the expanding radio source on the cluster gas.

The ROSAT HRI image of Cygnus A is shown in Fig. 10. This image reveals clearly the presence of the radio source within the cluster: X-ray emission from the hotspot regions, most of which is probably non-thermal and discussed below, deficits of X-ray surface brightness in the regions coincident with the inner parts of the radio lobes, and knots of excess X-ray emission along some of the edges of the radio source (see also Fig. 3 in Carilli et al. 1994b).

Clark and Harris present results from a 3D numerical simulation of the expected X-ray surface brightness distribution in the centers of clusters containing supersonically expanding radio sources such as Cygnus A. They show that the general anti-correlation between X-ray and radio surface brightness in Cygnus A within 35″ of the nucleus is consistent with the jet model for powerful radio galaxies. The deficits correspond to regions evacuated by the radio lobes, while the excesses correspond to emission from gas which has been displaced by the radio source. From the depth of the 'holes' in the X-ray gas at the positions of the radio lobes, they conclude that the radio source must effectively exclude the ICM, implying a contact discontinuity that is globally stable to mixing, and also that the transverse expansion of the shocked ICM must be substantial, otherwise the emission from the shocked gas would fill-in the observed holes. These conclusions are generally consistent with the analytic model of Begelman and Cioffi (1989) for shocked sheaths of ICM surrounding the lobes of powerful radio galaxies, in which they predict a width for the shocked ICM in Cygnus A $\geq 0.5\times$length of the lobes.

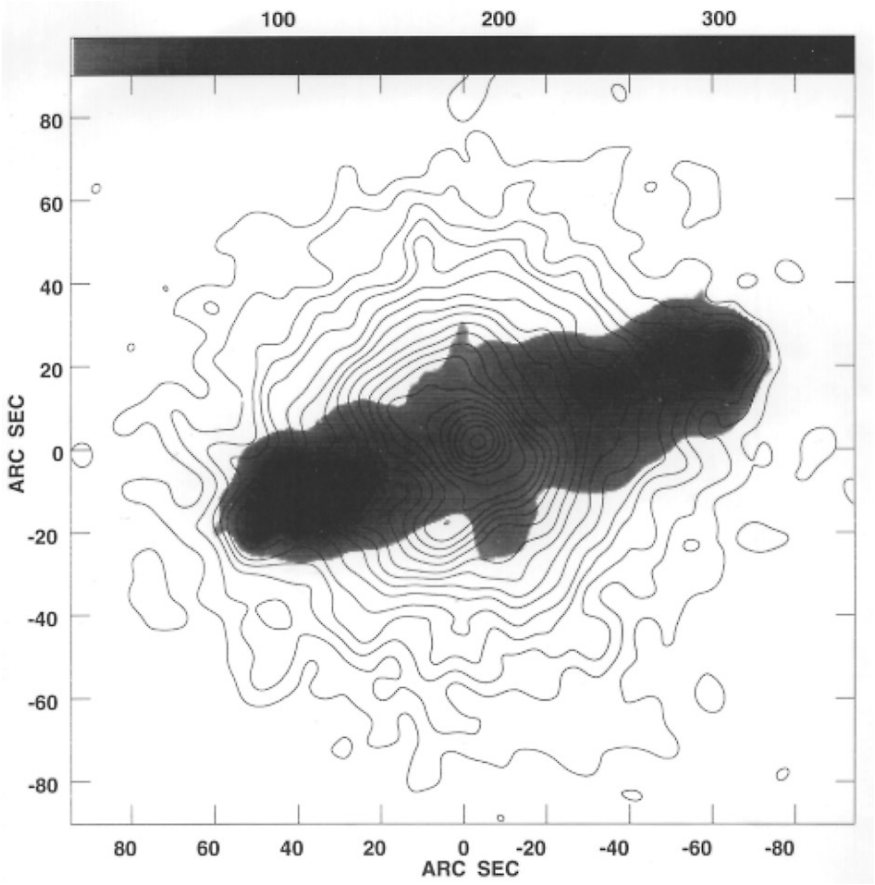

Fig. 10. The grey-scale is a radio image of Cygnus A at 327 MHz with 5″ resolution. The contours are from a ROSAT HRI observation of Cygnus A, reproduced from Carilli et al. (1994b), showing (predominantly) thermal X-ray emission from the inner regions of the Cygnus A cluster. Note that low surface brightness thermal X-ray emission continues to radii $\approx 10\times$ that shown on this image (Arnaud et al. 1984). The (presumably) non-thermal X-ray emission from the radio hotspot regions is also visible on this plot

Pressure balance

An important question is pressure balance of the various gaseous components in the cluster center (Arnaud et al. 1984, Carilli et al. 1994b, Alexander and Pooley 1996). At the hotspot radius of 60″ the pressure in the unperturbed ICM is 1×10^{-10} dyn cm^{-2}. The minimum pressures in the hotspots are 3×10^{-9}, while those in the higher surface brightness features in the heads of the radio lobes (beyond $\approx$ 45″ from the nucleus) are $\approx$ few$\times 10^{-10}$. Hence the hotspots are highly over-pressured relative to the external medium, and must be ram pressure confined. The external Mach number, M, for the hotspot advance can be calculated from the formula: $P_{HS}/P_{ICM} = (5M^2 - 1)/4$, derived from the standard Rankine-Hugoniot shock jump conditions in an ideal gas with ratio of specific heats = 5/3. For Cygnus A we obtain M = 5, implying an advance speed of 0.02c. The material in the heads of the lobes is mildly

over-pressured (factor of a few), and hence still requires ram pressure confinement, explaining the very sharp edges for the entire leading-surface of the radio lobes.

Within $20''$ of the cluster center the gas pressure has risen to $\geq 5 \times 10^{-10}$ dyn cm^{-2} (Reynolds and Fabian 1996). This is comparable to the pressure in the clumpy optical line emitting gas seen on kpc-scales for which pressures $\approx 8 \times 10^{-10}$ dyn cm^{-2} have been derived (Osterbrock 1989, Carilli et al. 1989b). This is also similar to the minimum energy pressure in the kpc-scale radio jet $\approx 6 \times 10^{-10}$ dyn cm^{-2}. However, the minimum pressure in the radio lobes is only 8×10^{-11} dyn cm^{-2}. Hence, the lobes within 15 h^{-1} kpc of the cluster center appear under-pressured relative to the thermal gas – a statement in conflict with the observed exclusion of the ICM from the radio lobes. The problem is worsened for an under-expanded lobe, in which case the sheath of shocked ICM enveloping the lobe would still be over-pressured relative to the unperturbed ICM (Begelman and Cioffi 1989). Carilli et al. discuss two possible solutions to this dilemma (see also Böhringer et al. 1993): either a significant departure from minimum pressure conditions in the radio lobes, or lobe pressures dominated by relativistic protons, with k $\geq$ 20. As pointed out above, such a departure from minimum energy conditions in the lobes could also solve the jet confinement problem.

While ROSAT has revealed evidence for the second dynamical component in Cygnus A as predicted by the jet model for powerful radio galaxies, significant questions remain concerning the interaction of the source with its environs, in particular concerning the bow shock at the leading edge of the lobe, and pressure balance between the radio bridge and the external medium. We expect that sensitive, spatially resolving spectroscopy with the next generation of X-ray satellites will delineate the density and temperature structure in the shocked ICM around Cygnus A in spectacular detail, thereby fulfilling the hopes of Begelman et al. (1984) of a fully constrained physical model for the dynamical evolution of a powerful radio source in a cluster atmosphere.

The X-ray hotspots

The ROSAT HRI image of Cygnus A has also revealed an excess of emission from the vicinity of the radio hotspots in both the northern and southern lobes (Harris et al. 1994a). Harris et al. show that these X-ray hotspots are compact and spatially coincident with the radio hotspots. The Galactic absorption corrected X-ray flux between 0.5 keV and 2 keV is 6.6×10^{-14} ergs cm^{-2} sec^{-1} for hotspot A, and 9.8×10^{-14} ergs cm^{-2} sec^{-1} for hotspot D.

Harris et al. consider, and reject, both thermal emission and an extrapolation of the radio synchrotron spectrum to very high energies for the X-ray hotspots. They conclude that the X-ray emission is most likely to be synchrotron self-Compton (SSC) radiation, i.e. up-scattering by the relativistic electrons of their own synchrotron radio photons. The combination of SSC emissivity and synchrotron emissivity allows them to derive the total energy density in relativistic particles and the energy density in the magnetic field independent of minimum energy assumptions. They calculate magnetic field strengths of $\approx$ 200 μG for the hotspot regions, close to the minimum energy value. They then argue that the agreement between minimum energy and SSC fields both supports the SSC interpretation for the X-ray hotspots, and suggests that conditions in the hotspots are close to equipartition. These conclusions hold for a small

value of k. If we assume that the pressures are dominated by relativistic protons, e.g. $k \geq 20$ (Böhringer et al. 1993), then the minimum energy fields increase by a factor ≥ 2.5, pushing them significantly higher than the SSC value.

Lastly, detecting SSC emission from the hotspots in Cygnus A provides independent evidence for a population of relativistic electrons, thereby confirming the original suggestion that the radio emission is synchrotron radiation (Shklovskii 1963) – a conclusion previously based solely on the high fractional polarizations and non-thermal power-law spectra observed in the radio.

The Cygnus A galaxy

Classification and cluster membership

From their plates taken with the 200-inch telescope Baade and Minkowsky (1954) identified Cygnus A as "an extragalactic affair, two galaxies in collision", drawing on the work of Spitzer and Baade (1951). Their plates showed a $m_{pg} = 17$ extragalactic nebula with two bright nuclear condensations, separated by 2 arcseconds, in position angle 115°. Despite the low galactic latitude, many extragalactic nebulae were seen in the vicinity of the Cygnus A galaxy. Baade and Minkowsky however could not simply classify the Cygnus A galaxy. Minkowsky was also puzzled by the double morphology of the radio source (Schmidt 1995). In 1957 he mentioned the interaction scenario again, and dealing with the radio components being located outside the optical galaxy he conjectured that "tidal filaments in some systems extend much farther" (Minkowski 1957). From Baade's original 200-inch plates Matthews et al. (1964) subsequently classified the galaxy as cD3 following Morgan (1958), with a double nucleus, and being the brightest member of a richness class 2 cluster. The cluster issue was taken up again by Spinrad and Stauffer (1982) who determined redshifts for six nearby E/S0 galaxies, and found four of these to be members of the Cygnus A group. The true richness class determination awaits high resolution, deep, wide-field CCD imaging and spectroscopy. Confirming earlier work by Yee and Oke (1978), the galaxy itself was found to have a normal (off-nuclear) gE or cD optical spectrum, and to be large: a reddening-corrected r(μ_R = 26) radius of 40 arcsec (40 kpc, for $H_0 = 75$) was measured (Spinrad and Stauffer 1982). The rather shallow surface brightness profile was however not confirmed by Pierce and Stockton (1986), Carilli et al. (1989), Vestergaard and Barthel (1993) and Stockton et al. (1995). These authors obtained good fits to the radial surface brightness profiles, at optical and near-IR continuum wavelengths, with de Vaucouleurs (1948) $r^{1/4}$ profiles, out to large radii. In that sense, Cygnus A may be different from the classical cD galaxies in rich clusters (e.g. Oemler 1976), having extensive envelopes. This recalls Thuan and Romanishin (1981) who found that brightest galaxies in poor clusters – of which Cygnus A may be an example – differ from cD galaxies in lacking such envelopes. This difference is commonly attributed to the low tidal stripping rate in poor clusters, and it will be of interest in this respect to determine the true Cygnus A cluster content. Against identification with a cD galaxy is the observation by Owen and Laing (1989) that cD galaxies tend to harbor twin jet FRI radio sources, and not classical double FRII sources such as Cygnus A, as well as the fact that the emission line properties of Cygnus A are somewhat atypical for cD galaxies (Baum et al. 1992). As long as new data do not show otherwise we prefer that Cygnus A be classified as

the brightest and largest elliptical galaxy in a poor cluster, but again, the true cluster content awaits determination.

Optical emission components

Whereas Baade and Minkowsky (1954) did notice that forbidden-line emission was strong, it took two decades until Van den Bergh (1976) investigated the Cygnus A galaxy in pure continuum light, and discovered that the double nature of the galaxy center and its resemblance to the Centaurus A galaxy NGC 5128 was mainly due to excess line and continuum emission in the 2 arcsec double morphology. The NW component of the double morphology stood out particularly with strong permitted and forbidden line emission. Subsequent astrometry located the radio core source in between this double optical feature (Kronberg et al. 1977). Later, high resolution optical imaging led to the discovery of a third compact optical emission feature coincident with the radio core (Thompson 1984). We will come back to this issue below, in the section on the nuclear regions.

Schmidt (1965) ranked Cygnus A as an extremely luminous line emitter in a study of powerful radio galaxies. The first extensive study of the emission line spectrum was carried out by Osterbrock and Miller (1975). This seminal spectrophotometric study of the central regions of the Cygnus A galaxy (aperture size $\approx 3''$) led to several important discoveries. First, the extinction as inferred from the emission line Balmer decrement was considerably greater than the extinction obtained from broad band aperture photometry (Sandage 1972). This was confirmed by Van den Bergh (1976) and Yee and Oke (1978). The Galactic foreground component was determined using field ellipticals (Van den Bergh 1976, Spinrad and Stauffer 1982). Osterbrock and Miller (1975) explained the measured extinction behavior in terms of additional extinction towards the central emission line regions in Cygnus A (later confirmed by Yee and Oke 1978). An extinction corrected optical continuum slope of -1.6 was determined, which is substantially harder than the value determined using the old reddening correction (Oke 1968). It is important to keep in mind that these data reflect the central regions of the Cygnus A galaxy. Second, the mass of the ionized gas in Cygnus A was determined to be about 10^7 $M_\odot$, the inferred filling factor was low, and the abundances were normal. Thirdly, the best candidate ionizing source appeared to be a non-thermal source of radiation, although a contribution of shock heating could not be ruled out. The extrapolation of the observed continuum ($L \propto \nu^{-1.6}$) fell short of producing the observed ionization, by 30%. This is a very important point, to which we will come back below.

Cygnus A became the prototype narrow-line radio galaxy (NLRG); see e.g., Osterbrock (1989). In contrast to other NLRGs however, stellar absorption features such as the calcium H and K lines were not seen. Yee and Oke (1978) had already established that a substantial component of nonthermal continuum contributed to the optical spectrum of Cygnus A, thereby diluting the stellar light. Osterbrock (1983) made the first attempt to quantify the relative contribution of this blue nonthermal continuum, also sometimes described as blue featureless continuum (BFC). He estimated the elliptical galaxy to contribute about 40% and the BFC to contribute about 60% around 5000Å in a $\approx 3''$ aperture. In summary, in the mid-eighties it was clear that a complex interplay was present in the Cygnus A galaxy, consisting of late type

stellar continuum, extended narrow emission line gas, blue featureless continuum and dust absorption/reddening.

Pierce and Stockton (1986) obtained line and continuum images as well as long slit spectroscopy in order to assess the relative contributions of the various optical components and to determine their morphology and origin. Their images confirmed and extended Van den Bergh's (1976) results, mapping out the morphology and ionization structure of the extended line emission at 1 kpc resolution. The emission line gas was found to have a clumped and filamentary structure. Just east of the NW emission line cloud, a fainter component coincident with the radio core was found. From its diluting effect on the stellar absorption features, the blue featureless continuum was found to extend over several arcsec in the central region, and ascribed to either a single obscured nucleus (via scattering) or many distributed photoionizing sources. The obscured nucleus model is particularly interesting in light of the proposal that powerful radio galaxies may harbor quasars in their nuclei, obscured by anisotropically distributed dust (Scheuer 1987, Peacock 1987, Barthel 1989), and recalls the Osterbrock and Miller (1975) finding that the extrapolated ultraviolet radiation fell short of producing the observed emission line radiation. Spatial reddening structure was measured, both in the line and in the continuum radiation. The presence of line-emitting filaments (Hα+[NII]), observed to stretch south and north-east for 5–10 arcsec was confirmed by Carilli et al. (1989). These authors compared emission line gas pressure values with radio synchrotron minimum energy pressures and found the gas to be overpressured except in the northern filament which seems to lie along the trailing edge of the eastern radio lobe. The same authors also determined the galaxy's absolute magnitude to be $M_R = -24$, confirming earlier claims that the object is very luminous. Typical line luminosity values are $\sim 10^{42}$ erg sec^{-1} (Carilli et al. 1989, Baum et al. 1989a). These values seem large, but Baum et al. (1989b) show that Cygnus A is somewhat underluminous for its radio luminosity. The [OIII] image obtained by Baum et al. (1988) shows the doubly ionized oxygen gas to be extended over $\sim$ 5 arcsec. This compares to $\sim$ 30 arcsec for the [OII] as inferred from the long-slit spectroscopy of Baade and Minkowsky (1954)! Confirmation of the extent of the [OII] nebula is however needed.

Infrared, submm, and mm emission

The line and continuum reddening mentioned above does not come as a surprise, since dust is abundant in the Cygnus A galaxy. IRAS data for Cygnus A and other radio galaxies were analyzed by Golombek et al. (1988), Knapp et al. (1990), and most recently Hes et al. (1995). The last authors plot 60μ luminosities as function of 178 MHz luminosities for the IRAS detected 3CR radio sources. Comparison of this plot (Fig. 11) with Fig. 1 suggests that although its 60μ luminosity is 2×10^{11} $L_\odot$ (within, but at the low end of the range for 3CR quasars), Cygnus A is anomalous in its radio rather than in its far-infrared emission. Barthel and Arnaud (1996) attribute the anomalously high radio luminosity of Cygnus A to comparatively strong radiation losses in the extended X-ray halo.

Dealing with the nuclear extinction in Cygnus A, Djorgovski et al. (1991) present the overall spectral energy distribution from its central component. It can be seen that most of the far-infrared emission must be thermal, and Djorgovski et al. (1991) fit a dust temperature of 75K. Depending on the poorly constrained submm spectrum, the

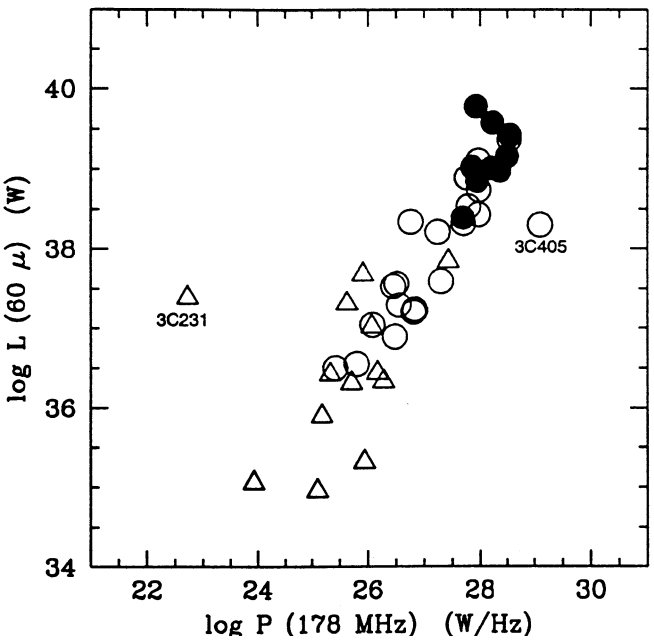

Fig. 11. Luminosities νL_ν of all 3CR radio galaxies and quasars detected at 60μ versus total radio power at 178 MHz, reproduced from Hes et al. (1995). Filled circles represent FRII quasars, open circles FRII radio galaxies, open triangles FRI radio galaxies. The marked sources are the starburst galaxy M 82 (3C 231) and Cygnus A (3C 405)

nonthermal far-infrared contribution can be estimated to be between a few and ten per cent.

Searches have also been made for CO emission from Cygnus A (Mirabel et al. 1989, Mazzarella et al. 1993, O'Dea et al. 1994, McNamara and Jaffe 1994), all unsuccessful. The most sensitive limits are by Mazzarella et al. (1993), who determine an upper limit to the mass in cold H_2 (using standard conversion factors) of 3×10^9 $M_\odot$. This upper limit to the cold molecular gas mass for Cygnus A is at the low end for masses seen in other radio galaxies (Mazzarella et al. 1993).

Considering the hot molecular gas, Ward et al. (1991) measure an unusually strong H_2 $\nu = 1 - 0$ S(1) emission line from Cygnus A, with a luminosity 1.0×10^{41} erg sec^{-1}, which brings Cygnus A close to classical star forming galaxies such as Arp 220 and NGC 6240. The implied mass of hot molecular gas leads to a mass ratio upper limit of hot/cold H_2 which is however not unusual. Ward et al. (1991) speculate that both X-ray heating and shock heating may be responsible for the H_2 excitation.

A merger origin for the Cygnus A galaxy?

Whereas merging is most likely an important mechanism triggering nuclear activity in galaxies (e.g., Heckman et al. 1986, Stockton 1990), there is only limited direct evidence that Cygnus A has gone through such a process. The well established $r^{1/4}$ surface brightness profile by itself does not exclude a recent merger (e.g. Schweizer

1982), but that fact combined with the absence of large scale tidal features and host distortion provides little evidence for a recent merger scenario. The best evidence that a merger may have taken place in Cygnus-A is in our view the detection by Stockton et al. (1994) of the secondary 2.2μ peak close to the bright nuclear emission line cloud (see Fig. 13) and of its peculiar nuclear gas kinematics (cf. Hernquist and Barnes 1991). Although the surplus of young stars in the nuclear regions does not require a merger origin, it is certainly consistent with it (Hernquist and Weil 1992).

Mazzarella et al. (1993) discuss how the activity in radio galaxies may be fundamentally related to starbursts, with both being triggered through a recent merger. Supporting evidence comes from the fact that many radio galaxies show peculiar morphologies, such as double nuclei and kpc-scale tails or shells, indicative of non-relaxed structures as expected in recent merger events (Heckman et al. 1986). Mazzarella et al. (1993) find that several nearby radio galaxies show CO emission, with implied H_2 masses between 5×10^9 and 5×10^{10} $M_\odot$, or one to seven times the H_2 mass of the Milky Way. For comparison, radio quiet far-infrared selected elliptical galaxies have H_2 masses 2 to 3 orders of magnitude lower than the Milky Way. This suggests rich supplies of molecular gas in radio galaxies. Moreover, radio galaxies show a similar correlation between L_{FIR} and $M(H_2)$ as starbursts, and the molecular mass-to-IR luminosity ratio for radio galaxies is in the range typical of nuclear starburst galaxies (15 to 100 $L_\odot/M_\odot$). Mazzarella et al. (1993) hypothesize that 'radio galaxies originate in colliding disk galaxies which evolve into gas-rich, peculiar E/S0 galaxies during the merger process.' Again, Cygnus A was not detected in CO emission, with the limit being at the low end for emission seen from nearby radio galaxies. Mazzarella et al. therefore speculate that Cygnus A may represent a dynamically old merger, having already processed a substantial gas mass of its parent disk galaxies. A larger, more homogeneous radio galaxy CO data base is needed to address this issue further.

It should be kept in mind that the estimated age of the radio source is $\approx 10^7$ years. It will be of interest to model a possible Cygnus A merging scenario taking the age of the radio source into account.

A cooling flow origin for the Cygnus A activity?

As mentioned above, ROSAT data suggest a mass cooling flow rate of ≈ 250 $M_\odot$ yr^{-1} for Cygnus A. Arguments pro and contra a cooling flow origin for the emission line gas in radio galaxies have been reviewed by Baum (1992). Also with reference to Baum et al. (1992) we here only mention that whereas a cooling flow origin for the gas cannot be excluded, Cygnus A is unusual in displaying high ionization gas and high radio luminosity, in combination with at most moderately ordered gas rotation (Tadhunter 1991, Stockton et al. 1994). This is at odds with the picture whereby the class of low luminosity/ionization radio galaxies are in cooling flow clusters and the high luminosity/ionization objects (such as Cygnus A) result from mergers, with the former displaying slow, ordered gas rotation and the latter fast, often large scale, rotation. However, while the optical spectrum of Cygnus A does show high ionization characteristics, it also has unusually strong low and intermediate ionization lines (e.g., Tadhunter et al. 1994). Also, Cygnus A may be a case where the observed gas kinematics is reduced by projection effects. Generally speaking, the issue of fueling the Cygnus A AGN (cooling flow or merger related) is still far from solved. There is little doubt that the high velocity gas observed both NW and E of

the nucleus (Tadhunter 1991, Stockton et al. 1994) is accelerated through jet–ISM interaction. As for the origin of this gas, both a merger and a cooling flow can be envisaged.

The nuclear regions of the Cygnus A galaxy

As discussed above, four components contribute to the optical radiation from the central regions of the Cygnus A galaxy. With central regions we mean here and in the following the central four by four arcseconds, as measured with respect to the central radio core, at RA(1950) 19:57:44.443, DEC(1950) +40:35:46.37. High resolution ground based optical images were recently obtained by Vestergaard and Barthel (1993), and Stockton et al. (1994). We reproduce in Fig. 12 three broadband images from the former authors, while dealing with the four contributing components: elliptical galaxy star light, narrow emission line gas, dust, and blue featureless continuum.

The V-band image, at 0.77arcsec resolution, shows that the Cygnus A nucleus is triple rather than double. The V-band is $\sim$ 40% contaminated with line emission (mostly [OIII]). It is seen that the NW-cloud which is known to be bright in line emission (Pierce and Stockton 1986) is resolved. An optical emission component appears coincident with the radio core component. There are strong gradients in the emission, which could be due to emission line gas, dust, ionization, or a combination of these. The intermediate level V-band morphology in this image – as well as in Thompson's (1984) 0.65arcsec resolution image – is nevertheless strikingly biconical. The R-band image, at 0.58arcsec resolution, shows the nuclear triple morphology in finer detail. The R-band is $\sim$ 45% contaminated with line emission (mostly Hα and [NII]). Both the NW line cloud and the nuclear component stand out, and both are clearly resolved. The central component appears to be located on a ridge, in p.a. $\sim 45^\circ$. Strong gradients are again seen. In contrast, the 0.80arcsec resolution I-band image, having at most 3% line contamination, is surprisingly smooth. There is a mild gradient from NW to SE, which is due to excess extinction NW, at the line cloud position. Patchy extinction may also be present 1 arcsec SE of the radio core position. A deconvolved I-band image at 0.42arcsec resolution (Vestergaard and Barthel 1993) shows two main extinction features ("dust fingers"): one in between the core component and the NW line cloud, entering from the north, and one just SW of the core component, entering from the south. These two features in combination are responsible for the faint continuum ridge at the radio core position. We recall that the presence of internal extinction in the central regions of the Cygnus A galaxy does not come as a surprise, since it was already inferred from the spectrophotometry (Osterbrock and Miller 1975, Pierce and Stockton 1986). Most of the excess emission at the radio core position seen in V- and R-band however, must be due to line emission. Increased reddening at this nuclear component was measured (Vestergaard and Barthel 1993).

The HST blue continuum and [OII] images of the nuclear region of Cygnus A (Jackson et al. 1994 and Cabrera-Guerra et al. 1996) confirm the presence of the optical component at the radio core location. Moreover, this component was found to lie on a faint bar in p.a. $\sim 45^\circ$, and to have at least a fifty-fifty line-continuum ratio. Another interesting finding was that the NW emission line line cloud appeared resolved into two separate line emitting components, with the radio jet passing through the gap in between. This gap is discussed in detail above.

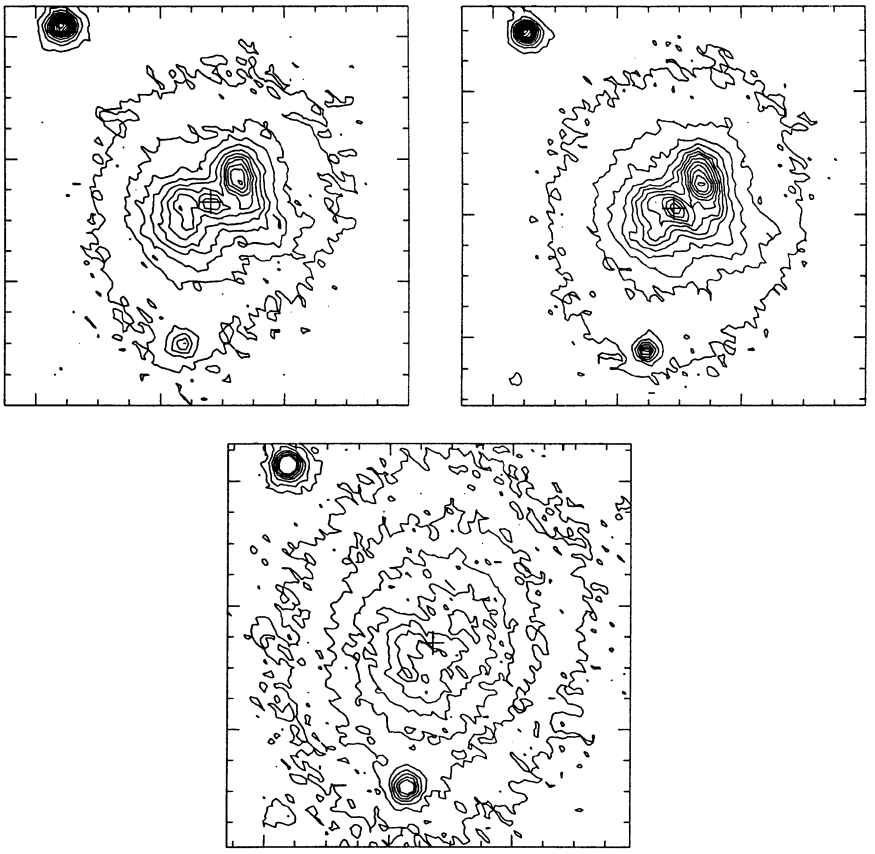

Fig. 12. V-, R- and I-band images of the central 12.8 × 12.8 arcsec in the Cygnus A galaxy, displayed at the same scale and centered on the (marked) radio core position. The tick marks are separated by 1 arcsec. The contour levels are: 19.44, 19.55, 19.66, 19.77, 19.88, 19.99, 20.14, 20.32, 20.53, 20.80, 21.15 and 21.67 mag per square arcsec (V-band), 18.25, 18.39, 18.53, 18.67, 18.81, 18.95, 19.09, 19.23, 19.39, 19.61, 19.88, 20.24 and 20.79 mag per square arcsec (R-band), and 18.77, 18.91, 19.08, 19.27, 19.50, 19.81, and 20.22 mag per square arcsec (I-band). Reproduced from Vestergaard and Barthel (1993)

Very recent ground based imaging in line and continuum radiation as well as spectroscopy was presented by Stockton et al. (1994). The nature of the featureless continuum was investigated using line-free images, subtracting symmetric galaxy profiles. The resulting spectral energy distribution is consistent with several mechanisms, but on the basis of the continuum light spatial distribution Stockton et al. (1994) find a starburst related origin the dominant one. Some level of scattered blue continuum must however be present, given the optical polarization measurements (Tadhunter et al. 1990). This issue will be dealt with in more detail in the next section. Spatial distributions of low and high ionization species were found to be different. In particular the Hα+[NII] were found to stretch outward N and S, in a $\sim$ 10arcsec planar structure perpendicular to the radio axis. Dust appeared associated with these low-ionization extensions. The high-ionization [OIII] does not show this N-S structure, but appears concentrated in a double morphology along the radio axis, centered on the radio core

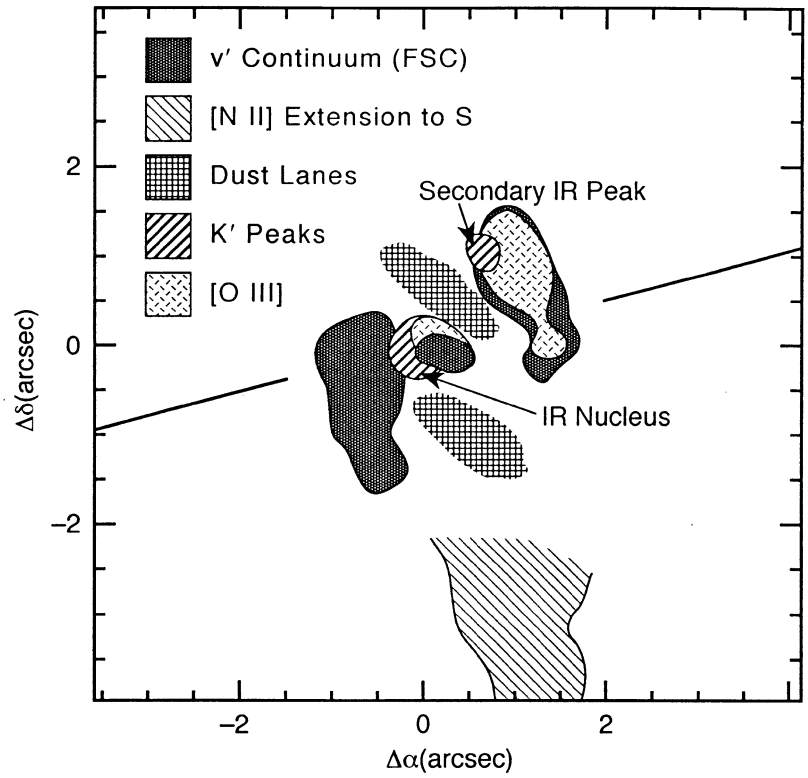

Fig. 13. Schematic diagram showing the major morphological components in the inner region of the Cygnus A galaxy. v' is a 1200Å wide line-free visual band with a substantial contribution from the (blue) flat-spectrum component (FSC), and K' is a 3500Å wide near-IR band centered at 2.11μ. The coordinates are centered on the IR/radio nucleus, and the diagonal line indicates the radio axis. Reproduced from Stockton et al. (1994)

position. A deconvolved [OIII] image confirms the presence of the gap in the NW cloud, as discovered on HST images as discussed above. Line ratio diagnostics indicate that the high-ionization species are almost certainly photo-ionized. Surprisingly, a Balmer decrement inferred extinction map shows little correlation with either the continuum or the emission line morphologies. On the basis of the observed absorption due to the MgIb triplet Stockton et al. (1994) obtain a Cygnus A heliocentric redshift value $z = 0.0562 \pm 0.00015$. The velocity field was found to be complex, with clear signs of counter-rotation, and high-velocity gas most likely associated with the radio jets, on both sides of the galaxy nucleus. The presence of such high-velocity gas had been noted earlier by Tadhunter (1991).

Using high signal to noise long slit spectroscopy, Tadhunter et al. (1994) also address the nature of the extended emission line system. Balmer decrements, observed with slits along and perpendicular to the radio axis, indicate significantly increased reddening at the radio core location, i.e., a piling up of dust at that position. This is in agreement with Vestergaard and Barthel (1993) and Stockton et al. (1994). Tadhunter et al. (1994) also discovered ionization gradients perpendicular to the radio axis, for several high-ionization lines. The measured horseshoe patterns are indicative

of an anisotropic ionizing continuum source with its axis aligned with the radio jet axis. Low-ionization gas was measured as far as 13″ south of the radio core position. This study as well as Stockton et al. (1994) show clearly that the sources of ionization for the low- and high-ionization lines are fundamentally different, although some difficulties in interpreting the ionization characteristics remain. For example, the extreme [NII] strength would argue for an as yet not understood substantially enhanced nitrogen abundance.

Shaw and Tadhunter (1994) investigated the nature of the featureless continuum, again by high S/N long slit spectroscopy. They measured its extent to be ~ 4 arcsec, aligned with the radio axis, and found it to contribute between 60% and 90% of the total ultraviolet flux. Stockton et al. (1994) point out that the actual fraction may be more uncertain. While it seems that the measurements are consistent with a scattering origin for the featureless continuum, the next section will illustrate that the situation is not that simple. The possibility of free-free emission being responsible for the featureless continuum (Antonucci et al. 1994) was dismissed by Stockton et al. (1994), on grounds of its surface brightness and spectral energy distribution. Figure 13, taken from Stockton et al. (1994) summarizes the above section, sketching the optical picture of the Cygnus A central regions.

An obscured QSO in Cygnus A?

Cygnus A might well be an important nearby example of a powerful radio galaxy harboring a QSO in its nucleus, confirming the (Fanaroff and Riley Class II) QSR – radio galaxy unification scheme (Scheuer 1987, Peacock 1987, Barthel 1989). Simply put, this scheme argues that FRII radio galaxies are the parent population of radio loud quasars, with the jets in quasars oriented closer to our line of sight than those in the radio galaxies. This scheme is based on the observation of weaker cores and jets and the larger angular sizes for radio galaxies as compared to quasars, coupled to their similar space density distributions, as well as the statistics of superluminal motion in these classes of objects. An essential ingredient is an opaque torus with a polar axis roughly aligned with the axis of the radio jet, obscuring the broad emission line region from direct view in the radio galaxy class. Although cone angle evolution (with redshift and/or luminosity) cannot be excluded, available data seem to imply a dividing cone angle of approximately 45° (Barthel 1989, Padovani and Urry 1991). Barthel (1993) and Urry and Padovani (1995) summarize arguments pro and contra this unification scheme.

As will be described below, a simple symmetric twin relativistic jet model suggests the Cygnus A radio source axis to be oriented at an intermediate angle to the line of sight, consistent with the simple FRII unification scheme. Tadhunter et al. (1994) point out that the opening half angle of the QSO cone in Cygnus A may be more like $\sim 60°$, with the radio axis inclination therefore greater than $\sim 60°$. In addition, we have seen that dust is abundant in the nuclear regions. In this respect it is also interesting to recall the study of Hes et al. (1993), investigating optical emission line luminosities and morphologies within the FRII unification scheme. Hes et al. (1993) find [OII] luminosities for the classes in accordance with the scheme, and infer larger sizes for the [OII] nebulae compared to the [OIII] nebulae, attributing these facts to dust in the narrow line region. Although [OII] images for Cygnus A have not been obtained, the original long slit spectroscopy of Baade and Minkowski (1954) indicated

an [OII] extent of at least 30 arcsec, which should be compared to $\sim$ 6 arcsec for the [OIII] nebula (Baum et al. 1988, Stockton et al. 1994)! However, proving that Cygnus A indeed contains a QSO obscured from direct view is another matter.

Following Pierce and Stockton's (1986) demonstration of an extended source of featureless blue continuum radiation, Goodrich and Miller (1989) presented spectropolarimetric measurements, in search for the nature of this continuum component. They observed a rather low percentage of polarization indicating that most of the blue light which Osterbrock (1983) had estimated to make up a large fraction of the light in the central regions does not arise via scattering, but is seen directly. Goodrich and Miller (1989) proposed that hot stars near the galaxy center must be responsible for the blue light component. Despite the low level of polarization, Tadhunter et al. (1990) were able to map the polarized V-band radiation, and discovered a polarization pattern indicative of bipolar reflection. This centro-symmetric pattern, which extended over the central 3 arcsec, was evidence that at least some part of the radiation was due to a continuum source obscured from direct view. This part (FC1, following Tran 1993) combines with directly seen blue radiation (FC2), possibly from hot stars, and the normal stellar population to make up the blue continuum in the central region of the Cygnus A galaxy. Near-infrared imaging by Djorgovski et al. (1991) and near-infrared spectroscopy by Ward et al. (1991) resulted in more evidence for the obscured QSO hypothesis. Whereas the former study reported a bright, very red nucleus at 2.2 and 3.7μ which could be combined with data at other frequencies for a rough extinction estimate ($A_V \sim 50 \pm 30$ mag), the latter study used established quasar correlations to obtain a more precise estimate for the nuclear continuum extinction: $A_V = 54 \pm 9$ mag. Recent near-IR imaging by Stockton et al. (1994) indicated the presence of a marginally resolved second K-band nucleus, located about 1 arcsec NW of the true (radio core) nucleus.

Hard X-rays could also penetrate through the postulated circumnuclear dust, and hence facilitate the search for an obscured QSO. The question of X-ray emission from the active nucleus of Cygnus A has been addressed both through spectroscopy, and high resolution imaging. Based on X-ray spectra taken with EXOSAT, Arnaud et al. (1987) were the first to discuss evidence for a hard X-ray tail to the spectrum of Cygnus A, perhaps indicative of emission from the active nucleus. Ueno et al. (1994) have recently obtained GINGA spectra of Cygnus A, confirming the results of Arnaud et al. (1987). For a single component thermal model they find an unreasonably high temperature of 18×10^7 K. The data is best fit using two-components: thermal emission from cluster gas at $T = 8.5 \times 10^7$ K, and a heavily absorbed ($N(HI) = 4 \times 10^{23}$ cm^{-2}) power-law emission component (presumably the nucleus) with photon index of 2 and total luminosity between 2 keV and 10 keV of 6×10^{44} h^{-2} erg sec^{-1}. These conclusions concerning the nuclear X-ray spectrum of Cygnus A are supported by recent ASCA observations (Arnaud et al. 1996). Although large, the total absorption corrected X-ray luminosity is somewhat smaller than that of radio-loud quasars of the same radio luminosity, being typically in the range 10^{45} – 10^{46} erg sec^{-1} (e.g. Zamorani et al. 1981). Harris et al. (1994b) find evidence for a point X-ray source at the center of Cygnus A on the ROSAT HRI image. This point source is robust in terms of modeling and subtracting the extended cluster distribution. On the other hand, using the the absorption column and core spectrum derived by Ueno et al. implies that the core source should be completely obscured in the HRI bandpass, i.e. the obscuring gas is opaque below about 4 keV. Investigation of the spectrum

of the compact X-ray core source must await future spatially resolving spectroscopic observations.

The absorption corrected X-ray luminosity for the nucleus of Cygnus A is furthermore comparable to that seen for broad line radio galaxies, and agrees with the rough correlation between far-infrared and hard X-ray emission for nearby broad-line AGN (Ward et al. 1988). Ueno et al. (1994) point out that the implied absorbing column density is very high, comparable to that found for some Seyfert 2 galaxies. The ultimate test of the existence of an obscured X-ray nucleus of quasar-type luminosity at the center of Cygnus A will be possible with the next generation of X-ray satellites, which will combine high spectral resolution with high spatial resolution.

Barvainis and Antonucci (1994) and McNamara and Jaffe (1994) searched for CO absorption towards the radio nucleus, arising in the postulated dusty molecular torus. Optical depth limits of ≈ 0.5 were set for both CO 0–1 and CO 1–2 at velocity resolutions of order 1 km sec^{-1}. The lack of CO absorption presents a challenge to the torus model for Cygnus A. Barvainis and Antonucci suggest three possible solutions. First, it may be that there is no such torus. Second, the sizes of the molecular clouds in the torus may be smaller than the size of the background continuum source. Models of Krolik and Begelman (1988) and Krolik and Lepp (1989) suggest cloud sizes $\approx$ 0.03 pc, which is still well below the smallest scale yet probed by VLBI observations. And third, Maloney et al. (1994) discuss the possibility that the radio continuum emission from the nucleus radiatively excites the CO, 'rendering the lower-J CO transitions undetectable in absorption.' This depends critically on the radio flux-to-particle density ratio, with high ratios leading to substantial radiative excitation. The extreme limit is a CO excitation temperature approaching the brightness temperature of the radio continuum nucleus. Current data cannot rule out any of these three options.

The most exciting recent result in the search for absorption towards the active nucleus of Cygnus A is the recent detection of HI 21cm absorption at the systemic redshift by Conway and Blanco (1995). The absorption line seen towards the nucleus is broad (FWHM = 270 km sec^{-1}), perhaps consisting of two components, with a peak optical depth of 0.05. These figures are in contrast to regular dust lane HI absorption: the NGC 5128 (Centaurus A) absorption for instance measures 30 km sec^{-1}. The implied neutral hydrogen column density towards Cygnus A is $2 \times 10^{19} T_S/f$, where T_S is the spin temperature of the gas, and f is the covering factor. Neither OH nor H_2CO absorption is detected, at 1% optical depth and 54 km sec^{-1} resolution. Conway and Blanco (1995) compare their results to absorption seen towards other radio loud AGN, and conclude that they are seeing absorption by the hypothesized dense circumnuclear torus. The opacity and velocity structure are comparable to those predicted by Krolik and Begelman (1988), and Krolik and Lepp (1989). Given the lack of molecular absorption, Conway and Blanco discuss the possibility of a dusty, *atomic* torus, and show that such a situation is physically reasonable, although a molecular torus is by no means precluded. Comparing their results to the X-ray studies, they suggest: $T_S = 10^4$ K, and f = 1, numbers which can be tested through future VLBI spectral line imaging.

A final curious point is that the spectrum of the VLBI nucleus is inverted between 5 GHz and 43 GHz. The straightforward interpretation of this inverted spectrum nucleus is synchrotron self absorption. However, it is worth noting that in their standard model for dusty molecular tori, Krolik and Lepp (1989) predict that such a torus will be optically thick to free-free absorption at around 10 GHz. If the inverted spectrum core is due to free-free absorption, then the width of the obscuring torus is set by

the fact that the inverted spectrum is seen only for the nucleus in Cygnus A, not the VLBI jet (Carilli et al. 1994a). The implied maximum width to the torus is ≈ 1 pc, in the case of torus axis oriented in the sky plane. This can be further tested with multifrequency VLBI observations.

Overall, it seems likely there is a continuum source of quasar-like luminosity in the nucleus of the Cygnus A galaxy, hidden from direct view by a dense column of dusty gas. Is there also an obscured broad emission line region? Ward et al. (1991), following earlier measurements by Saunders (1984) and Lilly and Hill (1987) determined a Paα line width of 510 km/sec, in good agreement with the optical Balmer line widths. More importantly, the extinction towards broad Paα emission was determined using the relationship between X-ray and broad line luminosity (Ward et al. 1988) resulting in $A_V(BLR) > 24$. It thus appears that even in the near-IR broad lines (as QSO characteristics) will be difficult to detect. In an attempt to determine the level of scattering using spectropolarimetry Jackson and Tadhunter (1993) found increased polarization towards the blue, but no sign of scattered broad lines, confirming similar work by Miller and Tran (1993). Stockton et al. (1994) examined their high S/N spectra in search for broad Hβ. The strong featureless continuum just SE of the radio core predicts broad Hβ equivalent widths of at least 50Å if all of the continuum is scattered QSO radiation. Stockton et al. (1994) measured an upper limit to such broad Hβ of 15Å, demonstrating that the featureless continuum is most likely not dominated by scattered QSO radiation.

A high S/N ultraviolet spectrum obtained with HST was presented by Antonucci et al. (1994). This spectrum, taken of the SE part of the Cygnus A nuclear region (which is dominated by continuum radiation) does show a broad MgII λ2795 line, with FWHM $\sim$ 7500 km sec^{-1} and equivalent width $\sim$ 25Å. Invoking a Rayleigh scattering origin ($\propto \lambda^{-4}$) or even a less steep scattering law, the measured MgII flux of 8×10^{-16} erg cm^{-2} sec^{-1} would be consistent with the absence in the optical band of broad Hα in available spectra. Also with reference to the ultraviolet polarization properties (Antonucci et al. 1994), these data comprise strong evidence that Cygnus A does harbour an obscured broad line region. It will be of great interest to compare the ultraviolet line and continuum polarization properties. Present Cygnus A data seem therefore to support the quasar-radio galaxy unification model. On the assumption of the (narrow) Balmer line emission to be due to quasar ionization Stockton et al. (1994) calculate the quasar blue magnitude to be $\sim$ 16. A similar computation by Metz et al. (1994) leads to $M_V \sim -23.5$ for the central QSO. It follows that the obscured QSO in Cygnus A may not be very luminous optically. We note however that some fraction of the featureless blue continuum and the line emission in the Cygnus A central regions may be due to young stars, so there is still uncertainty as to the true 'QSO content.' In fact, the quoted QSO luminosities are lower limits, since the adopted value of the ionization parameter is a lower limit, given the possibility of young stars contributing to the ionization of the gas.

The symmetric twin relativistic jet model applied to Cygnus A

The observation of superluminal motion in extragalactic radio jets has spurred the notion that these jets are moving relativistically. Doppler boosting due to relativistic motion has also been used to explain the observed one-sidedness of these jets, and the high surface brightnesses encountered (Kellermann and Pauliny-Toth 1981, Zensus

and Pearson 1990, Zensus and Kellermann 1994, Cawthorne 1991). The symmetric twin-relativistic jet model (STRJM) is an integral part of theories concerning the unification of powerful radio galaxies and quasars (e.g., Barthel et al. 1989, Antonucci 1993). Cygnus A provides an important test, since the jets in Cygnus A are thought to be close to the sky plane, as deduced from the large-scale morphology of the source (Hargrave and Ryle 1974, Scheuer 1983). The predictions are that for such a source the jet motion will be trans-luminal and the ratio of flux density in the jet to that in the counterjet will not be extreme.

The first VLBI images of Cygnus A revealed a pc-scale core source with a slight elongation along the axis of the kpc-scale source (Kellermann et al. 1981, 1975). This elongation was resolved into a core-jet by Linfield (1981) of $\approx$ 4 mas length. Further VLBI imaging revealed a 'knotty' jet extending 20 mas from the core source at the same position angle as the kpc-scale jet, and proper motion for one of the jet components was measured (Carilli et al. 1989b, 1994a).

The most recent VLBI studies of Cygnus A are by Sorathia et al. (1996) and Krichbaum et al. (1996). Both these studies detect a counterjet in Cygnus A. Sorathia et al. use three epochs of observations to determine the apparent velocity, β_A (in units of c), of the outermost jet component (J4) to be: β_A = 0.55$\pm$15 h^{-1}, and they find a value for the ratio of the integrated flux density in the jet to that in the counterjet, R, of: R = 5 $\pm$ 2 at 5 GHz. Using these two parameters (β_A and R), they apply the equations for the STRJM (Scheuer and Readhead 1979) to constrain the jet angle relative to our line of sight, θ, and to constrain the true jet velocity, β:

$$\beta_A = \beta sin\theta/(1 - \beta cos\theta)$$

and

$$\mathrm{R} = ((1 + \beta cos\theta)/(1 - \beta cos\theta))^{2-\alpha}$$

For h = 1/2 they find $1.0 \geq \beta \geq 0.6$ and $85^\circ \geq \theta \geq 50^\circ$. Hence, the jet in Cygnus A must be at an intermediate angle relative to our line of sight, and moving at a mildly relativistic velocity.

The higher resolution observations of Krichbaum et al. (1996) present a somewhat more complicated picture. The complexity and temporal variability of the sub-pc-scale structure makes core idenfication difficult. Making a nominal core identification with the most inverted spectrum component, Krichbaum et al. find evidence that the inner jet components may have a range in apparent velocities (β_A between 0.2 and 0.8 h^{-1}). This would be similar to the well studied case of the jet in M87 for which knot velocities ranging from sub- to superluminal have been observed (Biretta et al. 1995). Such an observation suggests that the apparent velocities represent a pattern speed, e.g. of surface waves on the jet, and not the true jet fluid velocity, thereby invalidating the standard STRJM analysis.

The central engine

Some theories

The most important unanswered questions in the study of powerful radio galaxies are: what is the ultimate source of energy? And why does a significant fraction of the energy released take the form of two highly collimated plasma beams? There has been a tremendous amount of theoretical work on these two related issues. For an exhaustive

early review of this subject see Begelman, Blandford, and Rees (1984), while a more recent treatment of these issues can be found in Wiita (1991), and Begelman (1993). We draw heavily upon these articles in what follows. Unfortunately, the observational constraints on these models remain mostly circumstantial and indirect. For the sake of completeness, we summarize a few of the basic theoretical points on central engine models, and present the observations of Cygnus A that may be relevant to these issues.

Most models for energy generation in AGN involve accretion onto a massive black hole at the center of the parent galaxy. The strongest argument for this idea remains that accreting black holes are extremely efficient at turning mass into energy. The gravitational energy released by in-falling material of mass, m, is roughly equal to the binding energy at the last stable orbit. Since this is roughly of order the Schwarzschild radius, $r_s = 2GM/c^2$, where M is the black hole mass, the energy released is a substantial fraction of the rest mass energy mc^2. Calculations for mass-to-energy conversion efficiency for accretion onto black holes yield 6% for non-rotating (Schwarzschild) holes, and 32% for maximally rotating (Kerr) holes. For comparison, nuclear fusion has a mass-to-energy efficiency $< 1\%$ (Wiita 1991). The gravitational energy released during infall is thought to be thermalized through the macroscopic viscosity supplied either by magnetic fields and/or turbulence. Other evidence for massive black holes in AGN include: variability of X-ray, optical, and radio nuclei on time-scales less that one day indicating a very small scale for the energy releasing region, and relativistic velocities in pc-scale jets indicating relativistic potential wells. Spectacular evidence for very centrally condensed masses in AGN has come from recent VLBI observations of rotating gas in the nucleus of NGC4258 showing a mass of $3.6 \times 10^7 M_\odot$ within 0.13 pc of the galaxy center (Miyoshi et al. 1995).

Models for the initial collimation of jets from accreting black holes typically involve either 'nozzles', 'funnels', or magnetically-focused beams. These different models depend on the form assumed by the accreting material, which in turn depends on the accretion rate. In all models the disks settle into orbits co-planar with the equator of the hole. The critical accretion rate is set by the Eddington limit = L_E/c^2, where L_E is the standard Eddington luminosity, $L_E = 1.3 \times 10^{38}\ M_{BH}$ ergs sec^{-1}, where M_{BH} is the mass of the hole in $M_\odot$. For subcritical accretion rates the radiation can be released efficiently at the disk surface, and a thin, rotating disk forms (i.e. the disk is 'cold' relative to the virial temperature). For critical accretion rates the photons heat the disk substantially, forming a 'thick disk', with temperature approaching the virial temperature. Such a disk will have narrow 'funnels' in the polar regions of non-stationarity (where a particle must either flow out, or fall in). For super-critical accretion rates the optical depth becomes such that the diffusion velocity for the photons is less than the in-flow velocity. In this case the hole is thought to be 'smothered', and the fluid and radiation field are in equilibrium. What may happen in this case is development of a quasi-spherical 'wind', where a wind is defined simply as material that has been heated (via photons or interactions with MHD waves) to the point that it can escape the gravitational potential.

The original 'beam' model of Blandford and Rees (1974) involved a hot, buoyant plasma injected into a flattened cloud of cooler gas. The hot gas 'percolates' through the denser gas via Rayleigh-Taylor instabilities. Steady flow patterns can be formed where the hot gas escapes from the cooler gas in the direction of the minor axis of the pre-existing gas cloud, forming a convergent-divergent 'de Lavall nozzle' with a minimum radius at the trans-sonic point (Norman et al. 1981). In fact, two oppositely directed outflows will form naturally, since the pressure in the hot 'bubble' is max-

imized at the position opposite the first jet. Blandford and Rees applied this model to Cygnus A, and predicted a nozzle forming at 200 pc from the nucleus. This is obviously not correct, given the collimated jet at sub-pc scales. However, the nozzle idea remains attractive in the case of quasi-spherical outflow in the super-critical accretion regime, in order to establish some form of initial collimation of the outflow. Models where nozzles form at distances $\leq$ few pc from the hole have been discussed in Norman et al. (1981) and Smith et al. (1983). These short, fat nozzles lead to fairly broad opening angles, and hence require some further focusing for the case of highly collimated radio jets as in Cygnus A.

Outflows from a thin disk driven by radiation pressure will most likely be very broad, and hence not applicable to radio jets. A similar argument can be used against winds from thin disks (Wiita 1991).

The narrow, deep funnels formed in thick disk models are obvious candidates for the formation of highly collimated outflows (Abramowicz and Piran 1980). Radiation pressure in these funnels will be both focusing, and outwardly accelerating. Due to Compton drag such radiation pressure driven jets are limited to form at radii of order 100 R_s, and are limited to bulk Lorentz factors ≤ 1.6 for a proton-electron plasma, and 4 for a pair plasma. Whether wind-type solutions work in the context of funnels remains to be demonstrated. Also, Wiita (1991) points out that even in the cases of deep, narrow funnels, the beams will be fairly broad (opening angles $\geq 10^\circ$).

Magnetic fields may play a fundamental role in the formation of highly collimated outflow from accreting massive black holes. One simple model involves a centrifugally driven outflow along magnetic field lines which are anchored to a rotating disk. If the emergent field at the disk surface makes an angle $\leq 60^\circ$ with respect to the outward radial direction, the charged particles will feel a centrifugal force larger than gravity, and fly outwards like beads on a string (Blandford and Payne 1982, Begelman 1993).

Another magnetic model for jet formation involves the creation of a thick 'ion-torus' in the case of sub-critical accretion. Such a torus will form if the infall time-scale is less than the cooling time. In this case the temperatures of the ions and electrons will decouple, with the ions having a temperature close to virial, giving rise to a thick 'ion-supported torus'. Since the accretion rate is low, the energy required to power the radio jets comes directly from the rotational energy of the hole, via the magnetic fields (Rees et al. 1982, Blandford and Znajek 1977). The polar fields are anchored to the hole, which behaves as a rotating conducting sphere. In the funnel region the fields 'wind-up', and a net-outward Poynting flux is generated, maintained by surface currents in the funnel walls. This Poynting flux becomes 'mass-loaded' (through e.g. pair production in the funnel zone), and the ensuing outflow may be collimated by the toroidal component of the magnetic field (Chan and Henriksen 1980, Blandford and Payne 1982). The attraction of this model for radio galaxies such as Cygnus A is that the rotational energy of the hole goes almost directly into the beam, and not into generating a strong optical or X-ray AGN. This model provides an alternative to the standard unification-by-orientation model: the quasar phase occurs when the accretion rate is high, while the radio galaxy phase occurs when the accretion rate is low.

Some observations: variability, small-scale structure

There are a few observations of Cygnus A which may be relevant to our understanding of the central engine. First is the simple fact that the jet is collimated and directed on scales ≤ 0.5 h^{-1} pc, and remains so out to 40 h^{-1} kpc.

A second important observable for the AGN in Cygnus A is variability. The radio nucleus has been observed over many years at many frequencies. Interferometric images at 90 GHz with arc-second resolution set an upper limit to core variability of $< 10\%$ on time-scales of both 10 months and 10 years (Wright and Sault 1993, Wright and Birkinshaw 1984). Likewise, imaging at 15 GHz with arc-second resolution at a number of epochs has detected no variability at the 10% level over 15 years (Carilli 1989, Alexander et al. 1984). Lastly, VLBI imaging at 5 GHz with 1 mas resolution reveals no variation of the inverted-spectrum nucleus, nor of the integrated flux from the core-jet, to a limit of 10% over 6 years, although individual knots in the jet may have varied by up to 40% (Carilli et al. 1994a).

Arnaud et al. (1987) mention possible variability of the hard X-ray (non-thermal) component in the nucleus of Cygnus A at about the 20% level over 6 months. Ueno et al. (1994) have reconsidered this possibility, and find no evidence for variability in hard, medium, or soft X-rays (20–10keV, 10–4 keV, and 4–2 keV, respectively) at the level of 10% on time-scales of 1 day to 1 month. Comparing their results with the previous hard X-ray results, Ueno et al. set a limit of less than a factor two variability on a time-scale of a few years.

Lastly, observations of structures on pc-scales in Cygnus A provide model dependent probes of the pressure in the nucleus of Cygnus A. The nucleus has a steeply rising spectrum of index > 0.9 between 5 GHz and 43 GHz (Carilli et al. 1994a, Krichbaum et al. 1993). If this rising spectrum is the result of synchrotron self absorption (SSA), a self-consistent model can be constructed from the SSA equation (Kellermann and Pauliny-Toth 1981), and the minimum energy equation. We assume $\nu_{\rm max}$ = 25 GHz, and use the observed flux density of the unresolved component of 0.7 Jy at 43 GHz (Krichbaum et al. 1993). The result is a nuclear size of 0.15 mas, and a core magnetic field of 0.16 G. The pressure in fields and particles is 10^{-3} dyn cm^{-2}. For comparison, the pressure in clouds in broad line regions of quasars is also thought to be of order 10^{-3} dyn cm^{-2}, or higher (Ulrich 1983). Hence the nuclear jet could be collimated by external pressure if a medium similar to that proposed for confining broad-line clouds in quasars exists in the core of Cygnus A. It should be noted that we have not considered relativistic beaming in the above calculations.

Overall, any model for the central engine in Cygnus A requires efficient conversion of energy into collimated outflow at a fair fraction of the speed of light starting on scales < 0.5 h^{-1} pc, while avoiding rapid variability of the non-thermal radio and X-ray luminosity of the AGN itself on time-scales up to 15 years. Also, the beam formation mechanism must maintain the jet direction to an accuracy of better than 20° over time-scales $\approx$ the radio source lifetime (of order 10^7 years). As pointed out by Wiita (1991) and Begelman (1993), extremely narrow beams on small scales suggest the fundamental involvement of magnetic forces as focusing agents, while the stability of the spin axis of a massive black hole is the logical origin for this long-term 'memory' of jet direction. The efficient model of Rees et al. (1982) for channeling the rotational energy of the black hole directly into collimated outflow on small scales via magnetic fields without generating tremendous waste heat in the process seems attractive in this regard.

We are still a long way from understanding the fundamental origin of the jets in Cygnus A. One glimmer of hope on the horizon is the advent of high frequency space VLBI, which will allow us to probe structure on scales $\approx 10^{17}$ cm in Cygnus A. While this is still about three orders of magnitude larger than the fundamental scale of the Schwarzschild radius, it approaches the scale of the hypothetical thick accretion disk and its associated funnels (Abramowitz and Piran 1980), and the general scale of the broad line region in quasars (Rees 1986).

Is Cygnus A representative of $z \sim 1$ radio galaxies?

In the introductory section the unique character of Cygnus A was noted, being more than 1.5 orders of magnitude more radio luminous than other nearby Fanaroff and Riley Class II radio galaxies. Due to the steepness of the radio luminosity function comparable radio galaxies are only found at redshifts 1 and beyond. Those extremely powerful distant radio galaxies are objects of great current interest, and the natural question arises if Cygnus A can be regarded as a nearby example. With reference to McCarthy (1993), many high redshift radio galaxies are characterized by very strong and extended (tens of kpc) narrow emission line regions, usually aligned with the radio source axis, blue optical-infrared colours, and spectacular continuum morphologies, again roughly aligned, with usually high level of optical (restframe ultraviolet) polarization. Whereas Cygnus A does have a blue excess this is concentrated in the nuclear region (central few kpc). Furthermore, neither the continuum nor the emission line morphologies are in any sense comparable to those seen in many high redshift radio galaxies, in their relation to the radio source. In addition, the inferred dust mass of $\sim 10^5$ – 10^6 $M_\odot$ (Djorgovski et al. 1991) is orders of magnitude below the values measured for some high redshift radio galaxies (e.g., Chini and Krügel 1994, Ivison 1995).

These facts, but more so the observation that Cygnus A is rather radio overluminous with respect to its far-infrared, optical and X-ray continuum emission, lead us to believe that Cygnus A is anomalously radio loud, and as such not representative of high redshift radio galaxies. Eales (1996) and Dunlop and Peacock (1995) indeed present evidence that some of the high redshift radio galaxy properties are correlated with the radio luminosity of the objects, rather than being a strong cosmological effect. Whereas we cannot rule out the possibility that some high redshift radio galaxies may also be anomalously radio loud and we eagerly await measurements in this respect, we feel (cf. Eales 1996) that evidence points towards classifying Cygnus A as truly a unique, remarkable source.

Acknowledgement. We would like to acknowledge NRAO for providing a pleasant atmosphere in Green Bank during the May 1995 Cygnus A Workshop, and Dan Harris, Dave Clarke, and Clive Tadhunter for commenting upon this work. CLC would like to thank R. Perley and J. Dreher for fostering his involvement in the study of Cygnus A. PDB acknowledges travel support from the Leids Kerkhoven-Bosscha Fund. We would also like to thank the various authors referenced in the figure captions for allowing reproduction of their figures. We made use of the NASA/IPAC Extragalactic Database (NED) which is operated by the Jet Propulsion Laboratory at Caltech, under contract with NASA/IPAC.

References

Abramowicz, M.A. and Piran, T. 1980, *ApJ* 241, L7.
Alexander, P. 1985, *MNRAS* 213, 743.
Alexander, P. 1987, *MNRAS* 225, 27.
Alexander, P. and Leahy, J.P. 1987, *MNRAS* 225, 1.
Alexander, P. and Pooley, G. 1996, in *Cygnus A: Study of a Radio Galaxy*, eds. C.L. Carilli and D.E. Harris (Cambridge: CUP), p. 149
Alexander, P., Brown, M.T., Scott, P.F. 1984, *MNRAS* 209, 851.
Antonucci, R.A. 1993, *ARAA* 31, 473.
Antonucci, R., Hurt, T., Kinney, A. 1994, *Nature* 371, 313.
Arnaud, K.A. 1996, in *Cygnus A: Study of a Radio Galaxy*, eds. C.L. Carilli and D.E. Harris (Cambridge: CUP), p. 51.
Arnaud, K.A., Fabian, A.C., Eales, S.A., Jones, C., Forman, W. 1984, *MNRAS* 211, 981.
Arnaud, K.A., Johnstone, R.M., Fabian, A.C. et al. 1987, *MNRAS* 227, 241.
Axford, W.I., Leer, E., McKenzie, J.F. 1982, *A&A* 111, 317.
Baade, W. and Minkowski, R. 1954, *ApJ* 119, 206.
Baars, J.W.M., Genzel, R., Pauliny-Toth, I.I.K., Witzel, A. 1977, *A&A* 61, 99.
Barthel, P.D. 1989, *ApJ* 336, 606.
Barthel, P.D. 1993, in *The Physics of Active Galaxies*, First Stromlo Symposium, eds. G.V. Bicknell, M.A. Dopita, P.J. Quinn, ASP Conf. Series 54, p. 175.
Barthel, P.D. and Arnaud, K.A. 1996, in preparation.
Barthel, P.D., Hooimeyer, J.R., Schilizzi, R.T., Miley, G.K., Preuss, E. 1989, *ApJ* 336, 601.
Barvainis, R. and Antonucci, R.A. 1994, *AJ* 107, 1291.
Baum, S.A. 1992, in *Clusters and Superclusters of Galaxies*, ed. A.C. Fabian (Cambridge: CUP), p. 171.
Baum, S.A., Heckman, T. 1989a, *ApJ* 336, 680.
Baum, S.A., Heckman, T. 1989b, *ApJ* 336, 702.
Baum, S.A., Heckman, T., Bridle, A., Van Breugel, W., Miley, G. 1988, *ApJS* 68, 643.
Baum, S.A., Heckman, T.M., Van Breugel, W. 1992, *ApJ* 389, 208.
Begelman, M.C. 1993, in *Astrophysical Jets*, STScI Symposium 6, eds. D. Burgarella, M. Livio, C.P. O'Dea (Cambridge: CUP), p. 305.
Begelman, M.C. and Cioffi, D.F. 1989, *ApJ* 345, L21.
Begelman, M.C., Blandford, R.D., Rees, M.J. 1984, *Rev. Mod. Phys.* 56, 255.
Bell, A.R. 1978, *MNRAS* 182, 147.
Bell, A.R. 1978, *MNRAS* 182, 443.
Bell, A.R. 1987, *MNRAS* 225, 615.
Benford, G. 1985, in *Physics of Energy Transport in Extragalactic Radio Sources*, eds. A.H. Bridle and J.A. Eilek (Greenbank: NRAO), p. 185.
Bicknell, G.V. and Henriksen, R.N. 1980, *Astrophys. Lett.* 21, 29.
Bicknell, G.V., Cameron, R.A., Gingold, R.A. 1990, *ApJ* 357, 373.
Biretta, J.A., Zhou, F., Owen, F.N. 1995, *ApJ* 447, 582
Birkinshaw, M. 1991, in *Astrophysical Jets*, ed. P.A. Hughes (Cambridge: CUP), p. 278.
Black, A.R.S., Baum, S.A., Leahy, J.P. et al. 1992, *MNRAS* 256, 186.
Blandford, R.D. 1996, in *Cygnus A: Study of a Radio Galaxy*, eds. C.L. Carilli and D.E. Harris (Cambridge: CUP), p. 264.
Blandford, R.D. and Rees, M.J. 1974, *MNRAS* 165, 395.
Blandford, R.D. and Znajek, R.L. 1977, *MNRAS* 179, 433.
Blandford, R.D. and Ostriker, J.P. 1978, *ApJ* 221, L29.
Blandford, R.D. and Königl, A. 1979, *ApJ* 232, 34.
Blandford, R.D. and Payne, D.G. 1982, *MNRAS* 199, 883.
Böhringer, H., Voges, W., Fabian, A.C., Edge, A.C., Neumann, D.M. 1993, *MNRAS* 264, L25.
Bolton, J.G. 1948, *Nature* 162, 141.
Bolton, J.G. 1982, *Proc. Astron. Soc. Aust.* 4, 349.
Bolton, J.G. and Stanley, G.J. 1948, *Nature* 161, 312.
Bridle, A.H., and Perley, R.A. 1984, *ARAA* 22, 319.
Bridle, A.H. and Eilek, J.A. (editors) 1985, *Physics of Energy Transport in Extragalactic Radio Sources*, NRAO, Greenbank, WV.

Bridle, A.H, Chan, K.L., Henriksen, R.N. 1981, *J. R. Astro. Soc. Can.* 75, 69.
Brinkman, A.C., Heise, J., Den Boggende, A.J.F., Grindlay, J., Gursky, H., Parsignault, D. 1977, *ApJ* 214, 35.
Burbidge, G.R. 1956, *ApJ* 124, 416.
Burbidge, G.R., Burbidge, E.M., Sandage, A.R. 1963, *Rev. Mod. Phys.* 35, 947.
Burch, S.F. 1979, *MNRAS* 186, 519.
Burgarella, D., Livio, M., O'Dea, C.P. (editors) 1993, *Astrophysical Jets*, STScI Symposium 6, Cambridge University Press, Cambridge.
Burn, B.J. 1966, *MNRAS* 133, 67.
Cabrera-Guerra, F., Pérez-Fournon, I., Acosta-Pulido, J., Wilson, A., Tsvetanov, Z. 1996, in *Cygnus A: Study of a Radio Galaxy*, eds. C.L. Carilli and D.E. Harris (Cambridge: CUP), p. 23.
Carilli, C.L. 1989, Ph.D. Thesis, Massachusetts Institute of Technology.
Carilli, C.L. 1996, in *Cygnus A: Study of a Radio Galaxy*, eds. C.L. Carilli and D.E. Harris (Cambridge: CUP), p. 76.
Carilli, C.L. and Harris, D.E. (editors) 1996, *Cygnus A: Study of a Radio Galaxy*, Cambridge University Press, Cambridge.
Carilli, C.L., Perley, R.A., Dreher, J.W. 1988, *ApJ* 334, L73.
Carilli, C.L., Dreher, J.W., Perley, R.A. 1989a, in *Hot Spots in Extragalactic Radio Sources*, eds. K. Meisenheimer and H.J. Röser (Heidelberg: Springer), p. 51.
Carilli, C.L., Dreher, J.W., Perley, R.A., Conner, S. 1989b, *AJ* 98, 513.
Carilli, C.L., Perley, R.A., Dreher, J.W., Leahy, J.P. 1991a, *ApJ* 383, 554.
Carilli, C.L., Bartel, N., Linfield, R. 1991b, *AJ* 102, 1691.
Carilli, C.L., Bartel, N., Diamond, P. 1994a, *AJ* 108, 64.
Carilli, C.L., Perley, R. Harris, D.H. 1994b, *MNRAS* 270, 173.
Cawthorne, T.V. 1991, in *Astrophysical Jets*, ed. P.A. Hughes (Cambridge: CUP), p. 187.
Chan, K.L. and Henriksen, R.N. 1980, *ApJ* 241, 534.
Chini, R., Krügel, E. 1994, *A&A* 288, L33.
Christiansen, W.A. 1989, in *Hot Spots in Extragalactic Radio Sources*, eds. K. Meisenheimer and H.J. Röser (Heidelberg: Springer), p. 291.
Clarke, D.A. 1990, in *Galactic and Intergalactic Magnetic Fields*, IAU Symp. 140, ed. R. Beck (Dordrecht: Kluwer), p. 403.
Clarke, D.A. 1992, in *Jets in Extragalactic Radio Sources*, eds. K. Meisenheimer and H.-J. Röser (Heidelberg: Springer), p. 243.
Clarke, D.A. and Burns, J.O. 1991, *ApJ* 369, 308.
Clarke, D.A. and Harris, D.E. 1996, in *Cygnus A: Study of a Radio Galaxy*, eds. C.L. Carilli and D.E. Harris (Cambridge: CUP), p. 199.
Clarke, D.A., Norman, M.L., Burns, J.O. 1989, *ApJ* 342, 700.
Clarke, D.A., Bridle, A.H., Burns, J.O. 1992, *ApJ* 385, 173.
Condon, J.J. 1992, *ARAA* 30, 575.
Conway, J.E. and Blanco, P.R. 1995, *ApJ* 449, L131.
Cox, C.I., Gull, S.F., Scheuer, P.A.G. 1991, *MNRAS* 252, 558.
DeGraff, D. 1992, PhD Thesis, Univ. of North Carolina.
DeGraff, D. and Christiansen, W. 1996, in *Cygnus A: Study of a Radio Galaxy*, eds. C.L. Carilli and D.E. Harris (Cambridge: CUP), p. 221.
De Vaucouleurs, G. 1948, *Ann. Astrophys.* 11, 247.
Dewhirst, D.W. 1951, in *Observatory* 71, 209.
DeYoung, D.S. 1991, *Science* 252, 389.
DeYoung, D.S. 1993, *ApJ* 405, L13.
DeYoung, D.S. and Axford, W.I. 1967, *Nature* 216, 129.
Djorgovski, S., Weir, N., Matthews, K., Graham, J.R. 1993, *ApJ* 372, L67.
Dreher, J.W. 1981, *AJ* 86, 833.
Dreher, J.W. 1985, in *Physics of Energy Transport in Extragalactic Radio Sources*, eds. A.H. Bridle and J.A. Eilek (Greenbank: NRAO), p. 109.
Dreher, J.W. and Feigelson, E. 1984, *Nature* 308, 43.
Dreher, J.W., Carilli, C.L., Perley, R.A. 1987a, *BAAS* 19, 731.
Dreher, J.W., Carilli, C.L., Perley, R.A. 1987b, *ApJ* 316, 611.
Drury, L.O'C. and Völk, H.J. 1981, *ApJ* 248, 344.

Eales, S.A. 1996, in *Cygnus A: Study of a Radio Galaxy*, eds. C.L. Carilli and D.E. Harris (Cambridge: CUP), p. 231.
Eilek, J.A. 1989, *AJ* 98, 256.
Eilek, J.A. 1995, *ApJ*, in press.
Eilek, J.A. and Shore, S.N. 1989, *ApJ* 342, 187.
Eilek, J.A. and Hughes, P.A. 1991, in *Astrophysical Jets*, ed. P.A. Hughes (Cambridge: CUP), p. 428.
Fabbiano, G., Doxsey, R.E., Johnston, M., Schwartz, D.A., Schwartz, J. 1979, *ApJ* 230, L67.
Falle, S.A. and Wilson, M.J. 1985, *MNRAS* 216, 79.
Fanaroff, B.L. and Riley, J.M. 1974, *MNRAS* 167, 31p.
Fomalont, E.B., Ebneter, K.A., van Breugel, W.J., Ekers, R.D. 1989, *ApJ* 346, L17.
Garrington, S.T., Leahy, J.P., Conway, R.G., Laing, R.A. 1988, *Nature* 331, 147.
Garrington, S.T., Conway, R.G., Leahy, J.P. 1991, *MNRAS* 250, 171.
Giacconi, R., Murray, S., Gursky, H. et al. 1972, *ApJ* 178, 281.
Golombek, D., Miley, G.K., Neugebauer, G. 1988, *AJ* 95, 26.
Goodrich, R.W. and Miller, J.S. 1989, *ApJ* 346, L21.
Hanbury-Brown R., Jennison, M.K., Das Gupta, M. 1952, *Nature* 170, 1061.
Hardee, P.E. 1996, in *Cygnus A: Study of a Radio Galaxy*, eds. C.L. Carilli and D.E. Harris (Cambridge: CUP), p. 113.
Hardee, P.E. and Norman, M.L. 1990, *ApJ* 365, 134.
Hardee, P.E. and Clarke, D.A. 1992, *ApJ* 400, L9.
Hardee, P.E. and Clarke, D.A. 1995, *ApJ* 451, L25.
Hargrave, P.J. and Ryle, M. 1974, *MNRAS* 166, 305.
Harris, D.E., Carilli, C.L., Perley, R.A. 1994a, *Nature* 367, 713.
Harris, D.E., Perley, R.A., Carilli, C.L. 1994b, in *Multi-wavelength continuum emission of AGN*, IAU Symposium 159, eds. T.J.-L. Courvoisier and A. Blecha (Dordrecht: Kluwer), p. 375.
Heavens, A. 1989, in *Hot Spots in Extragalactic Radio Sources*, eds. K. Meisenheimer and H.-J. Röser (Heidelberg: Springer), p. 247.
Heckman, T.M., Smith, E.P., Baum, S.A. et al. 1986, *ApJ* 311, 526.
Hernquist, L. and Barnes, J.E. 1991, *Nature* 354, 210.
Hernquist, L. and Weil, M.L. 1992, *Nature* 358, 734.
Hes, R., Barthel, P.D., Fosbury, R.A.E. 1993, *Nature* 326, 362.
Hes, R., Barthel, P.D., Hoekstra, H. 1995, *A&A*, 303, 8.
Hey, J.S., Phillips, J., Parsons, S. 1946, *Nature* 157, 296.
Hey, J.S., Parsons, S., Phillips, J. 1946, *Nature* 158, 234.
Hines, D.C., Owen, F.N., Eilek, J.A. 1990, *ApJ* 347, 713.
Hughes, P.A. (editor) 1991, *Astrophysical Jets*, Cambridge University Press, Cambridge.
Icke, Vincent 1991, in *Astrophysical Jets*, ed. P.A. Hughes (Cambridge: CUP), p. 232.
Ivison, R.J. 1995, *MNRAS* 275, L33.
Jackson, N., Sparks, W.B., Miley, G.K., Macchetto, F. 1994, *A&A* 284, 65.
Jaffe, W.J. 1980, *ApJ* 241, 924.
Jaffe, W.J. and Perola, G.C. 1974, *A&A* 26, 423.
Jafelice, L.C. and Opher, R. 1992, *MNRAS* 257, 135.
Jennison, R.C. and Das Gupta, M.K. 1953, *Nature* 172, 996.
Katz-Stone, D. and Rudnick, L. 1994, *ApJ* 426, 116.
Katz-Stone, D., Rudnick, L., Anderson, M. 1993, *ApJ* 407, 549.
Kardashev, N.S. 1962, *Sov. Astr.* 6, 317.
Kellermann, K.I. and Pauliny-Toth, I.I.K. 1981, *ARAA* 19, 373.
Kellermann, K.I., Clark, B.G., Niell, A.E., Schaffer, D.B. 1975, *ApJ* 197, L113.
Kellermann, K.I., Downes, A.J.B., Pauliny-Toth, I.I.K. et al. 1981, *A&A* 97, L1.
Kirk, J.G. 1989, in *Hot Spots in Extragalactic Radio Sources*, eds. K. Meisenheimer and H.-J. Röser (Heidelberg: Springer), p. 241.
Kirk, J.G. and Schneider, P. 1987, *ApJ* 315, 425.
Knapp, G.R., Bies, W.E., van Gorkom, J.H. 1990, *AJ* 99, 476.
Königl, A. and Choudhuri, A.R. 1985, *ApJ* 289, 173.
Krichbaum, T.P., Witzel, A., Graham, D.A. et al. 1993, *A&A* 275, 375.
Krichbaum, T.P., Alef, W., Witzel, A. 1996, in *Cygnus A: Study of a Radio Galaxy*, eds. C.L. Carilli and D.E. Harris (Cambridge: CUP), p. 92.

Krolik, J. and Begelman, M.C. 1988, *ApJ* 329, 702.
Krolik, J. and Lepp, S. 1989, *ApJ* 347, 179.
Kronberg, P. and Jones, T. 1982, in *Extragalactic Radio Sources*, IAU Symposium 97, eds. D. Heeschen and C. Wade (Dordrecht: Reidel), p. 157.
Kronberg, P., van den Bergh, S., Button, S. 1977, *AJ* 82, 315.
Laing, R.A. 1980, *MNRAS* 193, 439.
Laing, R.A. 1988, *Nature* 331, 149.
Laing, R.A. 1989, in *Hot Spots in Extragalactic Radio Sources*, eds. K. Meisenheimer and H.-J. Röser (Heidelberg: Springer), p. 27.
Laing, R.A., Riley, J.M., Longair, M. 1983, *MNRAS* 204, 151.
Leahy, J.P. 1991, in *Astrophysical Jets*, ed. P.A. Hughes (Cambridge: CUP), p. 100.
Leahy, J.P. and Williams, A. 1984, *MNRAS* 210, 929.
Leahy, J.P., Muxlow, T.W., Stevens, P.W. 1989, *MNRAS* 239, 401.
Lilly, S. and Hill, G. 1987, *ApJ* 315, L103.
Lind, K.R., Payne, D.G., Meier, D., Blandford, R.D. 1989, *ApJ* 344, 89.
Linfield, R. 1981, *ApJ* 244, 436
Linfield, R. 1982, *ApJ* 254, 465.
Longair, M.S. and Willmore, A.P. 1974, *MNRAS* 168, 479.
Longair, M.S. and Riley, J.M. 1979, *MNRAS* 188, 625.
Longair, M.S., Ryle, M., Scheuer, P.A.G. 1973, *MNRAS* 164, 243.
Lonsdale, C.J. and Barthel, P.D. 1986, *AJ* 92, 12.
Maloney, P.R., Begelman, M.C., Rees, M.J. 1994, *ApJ* 432, 606.
Mathews, A. 1989, in *Hot Spots in Extragalactic Radio Sources*, eds. K. Meisenheimer and H.-J. Röser (Heidelberg: Springer), p. 219.
Mathews, A. and Scheuer, P.A.G. 1991, *MNRAS* 242, 623.
Matthews, T.A., Morgan, W.W., Schmidt, M. 1964, *ApJ* 140, 35.
Mazzarella, J.M., Graham, J.R., Sanders, D.B., Djorgovski, S. 1993, *ApJ* 409, 170.
McCarthy, P.J. 1993, *ARAA* 31, 639.
McNamara, B.R. and Jaffe, W. 1994, *A&A* 281, 673.
Meisenheimer, K., Röser, H.-J., Hiltner, P. et al. 1989, *A&A* 219, 63.
Miley, G. 1980, *ARAA* 18, 165.
Miley, G.K. and Wade, C. 1971, *Astrophys. Lett.* 8, 11.
Miller, J.S. (editor) 1985, *Astrophysics of Active Galaxies and Quasi-Stellar Objects*, University Science Books, Mill Valley, CA.
Miller, J.S., Tran, H. 1993, *BAAS* 25, 919.
Mills, B.Y. 1952, *Aust. J. Sci. Research* A5, 456.
Mills, B.Y. and Thomas, A.B. 1951, *Aust. J. Sci. Research* A4, 158.
Minkowski, R. 1957, in *Radio Astronomy*, IAU Symp. 4, ed. H.C. van de Hulst (Cambridge: CUP), p. 107.
Minkowski, R. and Greenstein. J.L. 1954, *ApJ* 119, 238.
Mirabel, I.F., Sanders, D.B., Kazès, I. 1989, *ApJ* 340, L9.
Mitton, S. 1971, *MNRAS* 153, 133.
Mitton, S. and Ryle, M. 1969, *MNRAS* 146, 221.
Miyoshi, M., Moran, J., Herrnstein, J. et al. 1995, *Nature* 373, 127.
Morgan, W.W. 1958, *PASP* 70, 364.
Muxlow, T.W.B., Pelletier, G. Roland, J. 1988, *A&A* 206, 237.
Myers, S.T. and Spangler, S.R. 1985, *ApJ* 291, 52.
Norman, M.L. 1989, in *Hot Spots in Extragalactic Radio Sources*, eds. K. Meisenheimer and H.-J. Röser (Heidelberg: Springer), p. 193.
Norman, M.L. 1992, in *Jets in Extragalactic Radio Sources*, eds. K. Meisenheimer and H.-J. Röser (Heidelberg: Springer), p. 211.
Norman, M.L., Smarr, L., Wilson, J.R., Smith, M.D. 1981, *ApJ* 247, 52.
Norman, M.L., Smarr, L., Winkler, K.-H.A., Smith, M.D. 1982, *A&A* 113, 285.
O'Dea, C.P., Baum, S., Maloney, P., Tacconi, L., Sparks, W. 1994, *ApJ* 422, 467.
Oemler, A. Jr. 1976, *ApJ* 209, 693.
Oke, J.B. 1968, *AJ* 73, 849.
Osterbrock, Donald 1989, *Astrophysics of Gaseous Nebulae and Active Galactic Nuclei*, University Science Books, Mill Valley, CA.

Osterbrock, D.E. 1983, *PASP* 92, 12.
Osterbrock, D.E. and Miller, J.S. 1975, *ApJ* 197, 535.
Owen, F. 1989, in *Hot Spots in Extragalactic Radio Sources*, eds. K. Meisenheimer and H.-J. Röser (Heidelberg: Springer), p. 77.
Owen, F.N. and Laing, R.A. 1989, *MNRAS* 238, 357.
Pacholczyk, A.G. 1970, *Radio Astrophysics*, Freeman and Co., San Fransico.
Pacholczyk, A.G. 1977, *Radio Galaxies*, Pergamon Press, New York.
Padovani, P. and Urry, M. 1992, *ApJ* 387, 449
Peacock, J.A. 1987, in *Astrophysical Jets and their Engines*, ed. W. Kundt (Dordrecht: Reidel), p. 185.
Perley, R.A. and Taylor, G. 1991, *AJ* 101, 1623.
Perley, R.A. and Carilli, C. 1996, in *Cygnus A: Study of a Radio Galaxy*, eds. C.L. Carilli and D.E. Harris (Cambridge: CUP), p. 168.
Perley, R.A., Dreher, J.W., Cowan, J.J. 1984, *ApJ* 285, L35.
Pierce, M.J. and Stockton, A. 1986, *ApJ* 305, 204.
Porcas, R.W., in *Superluminal Radio Sources*, eds. J.A. Zensus and T.J. Pearson (Cambridge: CUP), p. 12.
Rees, M.J. 1978, *MNRAS* 184, 61P.
Rees, M.J. 1986, in *Quasars*, IAU Symposium 119, eds. G. Swarup and V.K. Kapahi (Dordrecht: Reidel), p. 1.
Rees, M.J., Begelman, M., Blandford, R., Phinney, E. 1982, *Nature* 295, 17.
Reid, M.J., Biretta, J.A., Junor, W., Muxlow, T.W.B., Spencer, R.E. 1989, *ApJ* 336, 112.
Reynolds, C. and Fabian, A. 1996, *MNRAS*, 278, 479.
Roland, J. and Hermsen, W. 1995, *A&A* 297, 9.
Roland, J., Pelletier, G., Muxlow, T.W.B. 1988, *A&A* 207, 16.
Röser, H.-J. 1996, in *Cygnus A: Study of a Radio Galaxy*, eds. C.L. Carilli and D.E. Harris (Cambridge: CUP), p. 121.
Röser, H.-J. and Meisenheimer, K. (editors), 1989, *Hot Spots in Extragalactic Radio Sources*, Springer-Verlag, Heidelberg.
Röser, H.-J. and Meisenheimer, K. (editors), 1992, *Jets in Extragalactic Radio Sources*, Springer-Verlag, Heidelberg.
Rudnick, L. and Katz-Stone, D. 1996, in *Cygnus A: Study of a Radio Galaxy*, eds. C.L. Carilli and D.E. Harris (Cambridge: CUP), p. 157.
Rudnick, L., Katz-Stone, D., Anderson, M. 1994, *ApJS* 90, 955.
Ruzmaikin, A., Sokoloff, D., Shukurov, A. 1989, *MNRAS* 241, 1.
Sandage, A. 1972, *ApJ* 178, 25.
Saunders, R. 1984, in *VLBI and Compact Radio Sources*, IAU Symposium 110, ed. R. Fanti, K. Kellermann, and G. Setti (Dordrecht: Reidel), p. 193.
Sarazin, C.L. 1986, *Rev. Mod. Phys.* 58, 1.
Sarazin, C.L. 1988, *X-ray emissions from clusters of galaxies*, Cambridge University Press, Cambridge.
Scheuer, P.A.G. 1974, *MNRAS* 166, 513.
Scheuer, P.A.G. 1982, in *Extragalactic Radio Sources*, IAU Symposium 97, eds. D. Heeschen and C. Wade (Dordrecht: Reidel), p. 163.
Scheuer, P.A.G. 1984, in *VLBI and Compact Radio Sources*, IAU Symposium 110, ed. R. Fanti, K. Kellermann, and G. Setti (Dordrecht: Reidel), p. 197.
Scheuer, P.A.G. 1987, in *Superluminal Radio Sources*, eds. J.A. Zensus and T.J. Pearson (Cambridge: CUP), p. 104.
Scheuer, P.A.G. and Williams, P.J. 1968, *ARAA* 6, 321.
Scheuer, P.A.G. and Readhead, A.C.S. 1979, *Nature* 277, 182.
Schmidt, M., 1965, *ApJ* 141, 1.
Schmidt, M., 1995, priv. comm.
Schweizer, F. 1982, *ApJ* 252, 455.
Shaw, M., Tadhunter, C. 1994, *MNRAS* 267, 589.
Shklovskii, I.S. 1963, *Sov. Astr.* 6, 465.
Siah, M. Javad 1985, *ApJ* 298, 107.
Siah, M. Javad and Wiita, P.J. 1990, *ApJ* 363, 411.
Simkin, S.M. 1977, *ApJ* 217, 45.
Slee, B. 1994, *Austr. J. Phys.* 47, 517.
Slysh, V.I. 1966, *Sov. Astr.* 9, 533.

Smith, F.G. 1951, *Nature* 168, 555.
Smith, F.G. 1984, in *The early years of Radio Astronomy*, ed. W.T. Sullivan, III (Cambridge: CUP), p. 237.
Smith, M.D. 1984, *MNRAS* 211, 767.
Smith, M.D., Smarr, L., Norman, M.L, Wilson, J.R. 1983, *ApJ* 264, 432.
Smith, M.D., Norman, M.L, Winkler, K.-H., Smarr, L. 1985, *MNRAS* 214, 67.
Sorathia, B., Bartel, N., Bietenholtz, M., Carilli, C., and Diamond, P. 1996, in *Cygnus A: Study of a Radio Galaxy*, eds. C.L. Carilli and D.E. Harris (Cambridge: CUP), p. 86.
Spinrad, H. and Stauffer, J.R. 1982, *MNRAS* 200, 153.
Spitzer, L. Jr., Baade, W. 1951, *ApJ* 113, 413.
Stockton, A. 1990, in *Dynamics and Interactions of Galaxies*, ed. R. Wielen (Heidelberg: Springer), p. 440.
Stockton, A., Ridgeway, S.E., Lilly, S.J. 1994, *AJ* 108, 414.
Stockton, A. and Ridgeway, S. 1996, in *Cygnus A: Study of a Radio Galaxy*, eds. C.L. Carilli and D.E. Harris (Cambridge, CUP), p. 1.
Swarup, G., Thompson, A.R., Bracewell, R.N. 1963, *ApJ* 138, 305.
Tadhunter, C.N. 1991, *MNRAS* 251, 46P.
Tadhunter, C.N., Scarrott, S.M., Rolph, C.D. 1990, *MNRAS* 246, 163.
Tadhunter, C.N., Metz, S., Robinson, A. 1994, *MNRAS* 268, 989.
Taylor, G., Barton, E., and Ge, J.-P. 1994, *AJ* 107, 1942.
Thompson, L.A. 1984, *ApJ* 279, L47.
Thuan, T.X. and Romanishin, W. 1981, *ApJ* 248, 439.
Tran, H. 1993, *BAAS* 25, 1440.
Tribble, P. 1993, *MNRAS* 261, 435.
Ueno, S., Koyama, K., Nishida, M., Yamauchi, S., Ward, M.J. 1994, *ApJ* 431, L1.
Ulrich, M.H. 1983, in *VLBI and Compact Radio Sources*, IAU Symposium 110, eds. R. Fanti, K. Kellerman, and G. Setti (Dordrecht: Reidel), p. 73.
Urry, C.M. and Padovani, P. 1995, *PASP* 107, 803.
Valtaoja, E. 1984, *A&A* 140, 148.
van den Berg, S. 1976, *ApJ* 210, L63.
van der Laan, H. and Perola, G.C. 1969, *A&A* 3, 468.
Vestergaard, M. 1992, MSc. Thesis, Copenhagen University.
Vestergaard, M. and Barthel, P.D. 1993, *AJ* 105, 456.
Ward, M.J., Done, C., Fabian, A.C., Tennant, A.F., Shafer, R.A. 1988, *ApJ* 324, 767.
Ward, M.J., Blanco, P.R., Wilson, A.S., Nishida, M. 1991, *ApJ* 382, 115.
Wentzel, D.G. 1969, *ApJ* 157, 545.
Wentzel, D.G. 1974, *ARAA* 12, 71.
Wiita, P.J. 1991, in *Astrophysical Jets*, ed. P.A. Hughes (Cambridge: CUP), p. 379.
Wiita, P.J. and Gopal-Krishna 1990, *ApJ* 353, 476.
Williams, A.G. 1985, Ph.D. Thesis, University of Cambridge.
Williams, A.G. 1991, in *Astrophysical Jets*, ed. P.A. Hughes (Cambridge: CUP), p. 342.
Williams, A.G. and Gull, S.F. 1985, *Nature* 313, 34.
Wilson, M.J. 1989, in *Hot Spots in Extragalactic Radio Sources*, eds. K. Meisenheimer and H.-J. Röser (Heidelberg: Springer), p. 215.
Winter, A.J.B., Wilson, D.M.A., Warner, P.J. et al. 1980, *MNRAS* 192, 931.
Wright, M.C., and Birkinshaw, M., 1984, *ApJ* 281, 135.
Wright, M.C. and Sault, R. 1993, *ApJ* 402, 546.
Yee, H.K.C. and Oke, J.B. 1978, *ApJ* 226, 753.
Zamorani, G., Henry, J.P., Maccacaro, T. et al. 1981, *ApJ* 245, 357.
Zensus, J.A. and Pearson, T.J. 1990, *Parsec Scale Radio Jets*, Cambridge University Press, Cambridge.
Zensus, J.A. and Kellermann, K.I., 1994, *Compact Extragalactic Radio Sources*, NRAO, Socorro, NM.

This article was processed by the author
using the Springer-Verlag TEX PJour1g macro package 1991.